Mesoscale variability study of the Agulhas Current from satellite radar altimetry and a high resolution model

Bjørn C. Backeberg

Degree Master of Science

University of Bergen
Norway

Mesoscale variability study of the Agulhas Current from satellite radar altimetry and a high resolution model

Bjørn C. Backeberg

M.Sc. Thesis in Physical Oceanography
May 2006

Geophysical Institute
University of Bergen

Abstract

Towards understanding the dynamics and eddy evolving processes in the greater Agulhas Current system, a Hybrid Coordinate Ocean Model (HYCOM) system has been set up to simulation the ocean circulation around Southern Africa in a hindcast experiment. In a region characterised by a general paucity of hydrographic observations, model validation from satellite remote sensing data products play an important role. In particular, radar altimetry observations from satellites are of beneficial use in the Agulhas Current regime, since it is known to exhibit some of the strongest mesoscale variability in the global ocean. Model validation from available in-situ data is presented with the focus on evaluating and implementing satellite altimetry data products for the purpose of validating the model mesoscale variability. An initial comparison of along-track sea level anomaly data from the Jason-1 satellite to merged gridded multi−altimeter data for the Agulhas Current suggested no significant loss of information in the generation of the merged maps. Thus allowing the use of the gridded data product in further model evaluation. It was found that the altimeter data provides good temporal and spatial comparisons, and as a by-product to the validation process, a frequency and variability study of the Agulhas Current regime was undertaken. Additionally to confirming strong seasonal signals in the region, they revealed that mesoscale eddies in the Mozambique Channel frequently interact at the Agulhas Retroflection. These observations are quantified statistically with the application of a Fourier analysis, which additionally provided a further method of validating the model simulation. The model simulation was able to represent the general characteristics of the circulation in the Agulhas regime, and supports many of the findings in the altimetry variability study. However, with the development of a large anticyclonic circulation feature upstream of the Agulhas Plateau in the current proper, the model simulation deteriorates in the later years. Available hydrographic data suggests a salinity deficit in the model fields, resulting in reduced baroclinic gradients, which in addition to other numerical instabilities may provide an explanation for the development of this feature. With continuously improving numerical schemes, increased computing power, and improved data assimilation techniques these models become increasingly realistic. As an oceanographic tool, the development of numerical models is vital, the first steps towards setting up and validating a regional HYCOM model for the oceans around Southern Africa are presented.

Acknowledgements

This work has been supported by the Mohn-Sverdrup Center for Global Ocean Studies and Operational Oceanography, through a private donation from Trond Mohn C/O Frank Mohn AS, Bergen.

Thank you to my supervisors, Prof. Johnny Johannessen and Dr. Laurent Bertino, for their support and integral input towards completing this project. Both of whom have committed a lot of their time in discussions and explanations, for which I am very greatful!

Thank you also to Belma Batlak, who provided the grid for the basin-scale model in which I was then able to nest the high resolution model of the Agulhas, and to Francois Counillon for providing an updated reading program for extracting the along-track sea level anomaly data.

I would like to thank the team at the Mohn-Sverdrup Center for endless patience and advice in teaching me the intricate details of numerical ocean modelling and its very many complications. In particular Dr. Nina Winther and Knut-Arild Lisæter, who have invested a lot of their time in answering my many (and frequent) questions.

Lastly, I would like to thank my family and friends for their support and patience throughout my extended absence from home.

Bjørn Christoph Backeberg

Bergen, Norway
May 2006

Contents

List of Figures

List of Tables

1 Introduction

Numerical ocean models play increasingly important roles towards understanding ocean dynamics and circulation. In the Agulhas Current this is of particular importance, since the dynamics of this region are not easily understood and explained. Furthermore, in a region where hydrographic data is sparse and operational observation systems limited, numerical models may play a vital role in ocean forecasting and decision making processes involved in determining dedicated research priorities.

In the 1980's the Agulhas Current was probably the least studied western boundary current in the world, and over the past decade, there has been increased interest in understanding the dynamics. Its characteristic extreme mesoscale temporal and spatial gradients, and the possibility of a very significant contribution to the global thermohaline circulation has motivated this recent research interest. Mesoscale variability, generally of the order of 100 to 500 km with temporal scales of one to a few months (Pond and Pickard, 1983), is generated by large-scale processes. However in a feed-back mechanism, it provides significant input to the general large scale circulation and its dynamics are important to understand in this regard.

To this end, the Hybrid Coordinate Ocean Model (HYCOM; Bleck (2002); Figures 1 and 6) has been set up to simulate the greater Agulhas Current system, in an effort to improve the understanding of its flow dynamics and mesoscale variability. In order to use a numerical modelling system in focussed process studies, a systematic validation has to be undertaken to ensure the relative accuracy of the simulation.

Satellite remote sensing over the past years has developed to a stage where high resolution observations of the ocean surface are possible at near global scales. The Agulhas Current system is characterised by a general paucity of hydrographic observations and these remotely sensed observations provide a powerful tool for measuring the oceans here.

As temporal and spatially more complete data sets become available, these data provide a useful means for model validation, frequency and variability studies. In particular, satellite altimetry, providing information regarding the height of the sea surface, and its anomaly, is becoming increasingly instrumental in describing the mesoscale dynamics of the ocean at high resolutions. Additionally, with the merging of multiple satellite altimeter data in improved mapping techniques (Ducet et al., 2000), these data allow for improved approaches in global and regional ocean studies.

The dynamics and characteristics of the greater Agulhas Current system display strong temporal and spatial gradients, making it a particularly attractive region to study from radar altimetry. Its mesoscale variability is well captured in the sea level anomaly (SLA) fields provided.

Results from a first hindcast simulation experiment of HYCOM for the region are presented, and its validation against available in-situ and remote sensing data. Because of limited hydrographic data in the area and its strong mesoscale gradients, the focus of this study revolves around evaluating and implementing SLA data, derived from satellite altimeters, for the purpose of model validation. The analysis method applied in model validation further allowed for variability studies of the region, and many of the findings are subsequently supported by the model simulation.

The paper is organised as follows. A general description of the regional flow dynamics is given in Chapter 2. The initial evaluation of the altimeter data for the Agulhas Current region is outlined in Chapter 3, where along-track SLA data is compared to *monthly mean* gridded SLA data in an attempt to quantify the loss or smoothing of information in the merging of multiple altimeter data into gridded fields. The HYCOM model system is described in Chapter 4, and the model simulation of the Agulhas Current system flow dynamics is described from surface velocity fields in Chapter 5. Validation of the model system against available in-situ and remote sensing data is presented in Chapter 6. Chapter 6.3 focusses on using satellite altimeter derived SLA data in quantitative model validation and variability studies for the Agulhas Current region. Further uses of SLA data in model validation in terms of eddy kinetic energy is outlined in Chapter 7 and the most significant findings and conclusions of this study are summarised in Chapter 8.

2 The greater Agulhas Current system

The Agulhas Current has been described as one of the strongest western boundary currents in the world's oceans. Forming part of the South-West Indian Ocean sub-gyre, the current flows polewards along the southeastern coast of Southern Africa between 27 °S and 40 °S (Gordon (1985); Stramma and Lutjeharms (1997)).

The greater Agulhas Current system (Figure 1) can be divided into five distinct sub-regions, each region displaying specifically different flow dynamics, and each contributing in a different manner towards the flow dynamics and mesoscale variability of the Agulhas Current regime: The source regions, the Agulhas Current, the Agulhas Retroflection, the Agulhas Return Current and the Southern Ocean. These sub-regions will be discussed in more detail below.

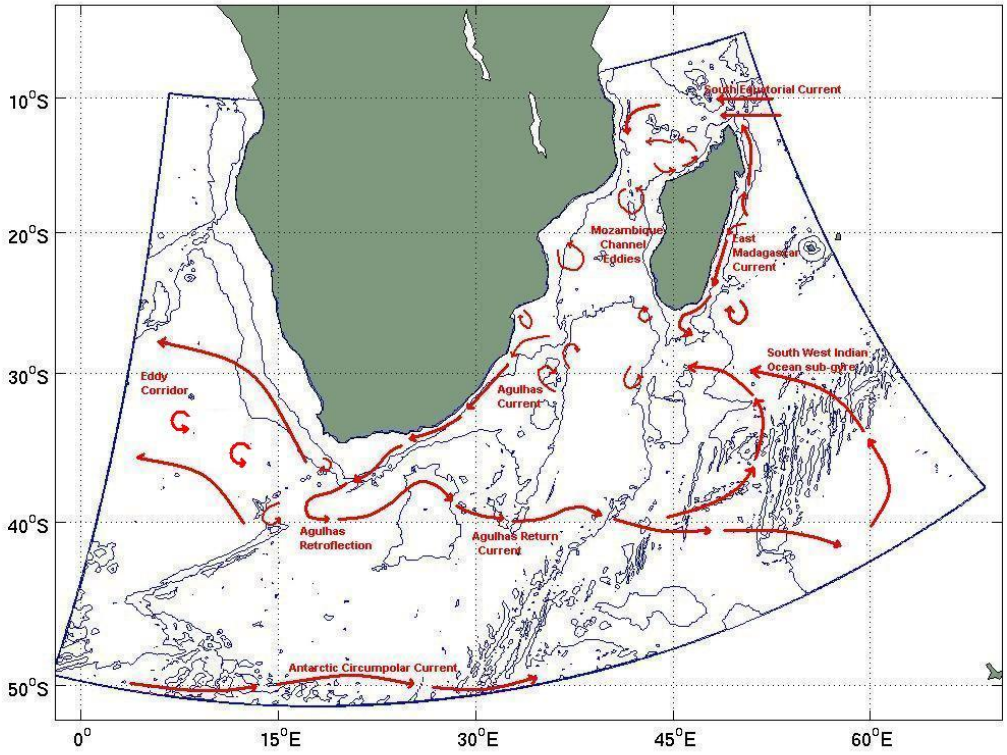

Figure 1: *HYCOM model grid and bathymetry, with conceptual major circulation features of the greater Agulhas Current system. Adapted from Lutjeharms (2006).*

2.1 Source regions

The Agulhas Current is thought to have two main sources, the South Equatorial Current (SEC), and recirculation from the South-West Indian Ocean sub-gyre, which supplies the greater part: 40 Sv of a total 60 Sv in the upper 1000 m (Stramma and Lutjeharms, 1997).

Previously the classical portrayal of the ocean circulation in the South-West Indian Ocean has been described as a bifurcation in the SEC upon its arrival at the East Madagascar Coast, into a northern and southern branch. The latter flowing poleward along the East Madagascar Coast as the East Madagascar Current (EMC). The northern branch carries the remainder of the SEC past the northern tip of Madagascar towards the African East Coast, where the current again splits, flowing north forming the Somali Current, and south into the Mozambique Channel.

It was thought that the flow through the Mozambique Channel and poleward along the East Madagascar Coast occurred in the form of western boundary currents, which converge somewhere off the coast of South Africa to form the Agulhas Current. These concepts were based on analyses of ship drift data, e.g. Sætre (1985) and Lutjeharms et al. (2000), and have since been shown to be incorrect, especially in respect of the flow in the Mozambique Channel.

This region can in general be charactarised as an area with scarce hydrographic observations, and much of the knowledge is derived from modelling studies, satellite remote sensing, and few dedicated research cruises.

2.1.1 Mozambique Channel

The flow in the Mozambique Channel as it is known today, is dominated by southward progressing anticyclonic eddies (Sætre and da Silva (1984); Biastoch and Krauss (1999) and de Ruijter et al. (2002)), contrary to previous descriptions of a continuous, unbroken western boundary current. These eddies drift southward along the shelf at approximately 4.3 kilometers per day, and may eventually reach the Agulhas Current (Schouten et al., 2002).

Flow in the remainder of the channel is thought to be sluggish and quite variable (Sætre, 1985). Modelling studies have suggested residual monsoonal effects in the Mozambique Channel, e.g. Maltrud et al. (1998), but there have been no observations to support these findings.

2.1.2 East Madagascar Current and its Retroflection

Along the eastern shore of Madagascar, the shelf is narrow, with a steep continental slope. The split into the northern and southern branches of the EMC occurs between 17 °S and 18 °S, at the Madagascar East Coast. The poleward flowing EMC has been described as a small intense western boundary current, with speeds reaching 0.66 $m.s^{-1}$, extending 50 km offshore. Similar velocities have been observed in the northern branch (Lutjeharms et al., 2000)

Lutjeharms et al. (1981) observed a retroflection of the EMC south of Madagascar, similar to the Agulhas Retroflection, generating cyclonic and anticyclonic eddies which drift westwards towards Africa (de Ruijter et al., 2004). A retroflecting EMC implies a reduced and episodal contribution to the Agulhas Current.

2.2 Agulhas Current

Following from previous descriptions of the Agulhas Current sources, the Mozambique Channel eddies and the EMC do not form a continuum with the Agulhas Current. However, it seems that they both affect its dynamics (Lutjeharms, 2006).

The Agulhas Current itself has distinctly different characteristics in its northern extents compared to its southern reaches.

2.2.1 Northern Agulhas Current

The northern Agulhas Current is characterised by very strong, and stable flow conditions. At its fully constituted state, near 28 °S, the current course closely follows the narrow continental shelf (Gründlingh, 1983), meandering less than 15 km from its mean path. More recently, year long direct current observations from moorings at 31 °S, have shown the current to lie within 31 km from the coast almost 80% of the time, with an average total poleward transport of 69.7 Sv (Bryden et al., 2005). Surface current velocities in the Agulhas Current have been estimated to reach up to 2 $m.s^{-1}$.

The dominant mode of variability in the northern Agulhas Current occurs in the form of intermittent cyclonic meanders, known as "Natal Pulses". These form at the Natal Bight, located close to the South African Coast between 29 °S and 30 °S. Here the continental slope is gentler and the shelf wider (Lutjeharms and Roberts, 1988), allowing for inshore cyclonic circulation, which eventually develops into a Natal Pulse. These meanders form approximately six times per year and propagate downstream at rates of $\sim$10 $km.d^{-1}$. It is thought that their southward progression and resultant interaction at the Agulhas Retroflection is associated with Agulhas Ring shedding events (van Leeuwen et al., 2000).

2.2.2 Southern Agulhas Current

Contrary to the northern Agulhas Current, the flow in the southern regions displays characteristics more typical of western boundary currents. With a separation of the continental shelf from the coast near 35 °S, the current begins to exhibit numerous meanders, plumes and eddies (Lutjeharms et al., 1989).

The average current trajectory follows the shelf edge southwestwards along the Agulhas Bank. With the southern termination of the Agulhas Bank, south of Cape Agulhas, the current continues on its southwesterly path, developing oscillations of increasing amplitude until it eventually retroflects near 40 °S and between 16 °E and 20 °E.

2.3 Agulhas Retroflection

The Agulhas Retroflection exhibits some of the highest levels of mesoscale variability in the world's ocean (Lutjeharms and van Ballegooyen (1988); Garzoli et al. (1996)). The retroflection loop may have a diameter of up 340 km, and shedding of anticyclonic retroflection eddies, or "Agulhas Rings", occurs here at irregular intervals (Lutjeharms and van Ballegooyen, 1988). These Agulhas Rings are unique because they form in association with a *zonal* protrusion of the parent current (Pichevin et al., 1999), and are typically larger than rings formed in association with current and frontal instabilities, e.g. Gulf Stream and Kuroshio rings.

The geographical position of the retroflection is not stationary. It propagates westward at rates varying between 7 and 15 km.d^{-1} (Olson and Evans, 1986), with Agulhas Rings occluded at its western extremity before retrograding eastward.

Agulhas Rings may have diameters of 200 to 280 km, and reach depths of 1100 m, making them some of the largest eddies to be observed in the global oceans. They drift into the South Atlantic Ocean at 5-8 km.d^{-1}, in a general northwesterly direction from the retroflection. Numerical experiments (Pichevin et al., 1999), show that ring generation from a retroflecting current is an inevitable event, where rings form to compensate for a zonal momentum flux. Additionally, they showed that there is no obvious numerical relationship between the presence of Natal Pulses and the production of rings, as has been suggested by observations.

The process of ring shedding from the Agulhas Current remains to this day not entirely understood.

2.4 Agulhas Return Current

Following the Agulhas Retroflection, the core of the current returns eastward in the Agulhas Return Current. It flows towards the South-Indian Ocean between 38 °S and 40 °S, with a tendency to gradually flow at higher latitudes further east (Lutjeharms and Ansorge, 2001). Its core width has been described to be around 70 km wide with flow velocities up to 2 m.s^{-1} evident, transporting a volume of 44 $\pm$ 5 Sv in the upper 1000 m.

Quasi-stationary meanders have been observed in the Return Current flow (Belkin and Gordon, 1996), their southern "crests" found predominantly near 29.7 °E, 35.5 °E and 42.9 °E (Boebel et al., 2003b). The first of these meanders is topographically induced, flanking the Agulhas Plateau around 25 °E and 29 °E, although modelling studies neglecting detailed bathymetry (Pichevin et al., 1999) also produce a similar meander east of the Agulhas Retroflection, suggesting an additional dynamical mechanism for the presence of this feature.

2.5 Southern Ocean

For the purpose of this study and as the last of the five sub-regions, a description of the Southern Ocean north of 50 °S and between 0 °E and 60 °E, which is covered by our model domain follows.

The Southern Ocean between Africa and Antarctica is dominated by frontal bands (Lutjeharms, 1985). These fronts form from a northward Ekman transport component arising from the Coriolis effect upon the eastward flowing Antarctic Circumpolar Current (ACC). They are defined as regions where convergence (and downwelling) or divergence (and upwelling) occurs. Three main frontal bands are evident in our study area: the Subtropical Convergence (STC), the Subantarctic Front (SAF) and the Antarctic Polar Front (APF).

The STC is the northern most front in the Southern Ocean, with a mean latitudinal position around

41 °S. Here cold dense Subantarctic water subducts beneath warm Subtropical waters, forming Central Water masses. Of the three main frontal bands mentioned, the STC displays the strongest temperature and salinity gradients, ranging from 10 °C to 18 °C and 34.3 to 35.5 psu at the surface (Belkin and Gordon, 1996).

The SAF marks the northern boundary of the Polar Frontal Zone and the southern extent of the Subantarctic Surface Water. Contrary to the STC, with its sharp horizontal gradients, the SAF is less distinct in its surface salinity and temperature expression, but can generally be found around 47 °25 ′S.

Further south lies the APF, but its mean position near 50 °47 ′S is not always captured in our model and study domain. It marks the location where Antarctic Surface Water subducts and moves northwards gradually deepening to form Antarctic Intermediate Water.

3 Satellite Altimetry

Recent developments in satellite remote sensing and microwave radiometry provide useful means to measure ocean surface structures and variability on a global scale at high temporal and spatial resolutions (Robinson, 2004). In particular measurements from satellite altimeters provide physical information about ocean phenomena such as fronts, currents, eddies, and other features associated with ocean circulation (Rouault and Lutjeharms, 2003).

In the context of operational oceanography, which aims to provide routine marine information to government, industry, commercial and public users, satellite remote sensing plays an important role. Ocean measurements from satellites, allow for broad temporal and spatial coverage, and may be used in validation and data assimilations of ocean models, which provide ocean state forecasts for interested parties, such as shipping industries, offshore industries and harbour authorities.

Marine information is provided in a broad spectrum of services and products. Ranging from climate information for design and long term operational planning, in the coastal and offshore industries, to short term nowcast / forecasts used in supporting disaster mitigation operations, such as oil spills. Ships have also been known to make use of strong ocean currents to optimise their operations at sea, "riding" the current to lessen both the travel time and fuel consumption.

Satellite altimeters are nadir-pointing radars. They emit regular pulses and measure the travel time, magnitude and shape of each return signal, which is reflected from the Earth's surface. Over the ocean, these primary observations are used to estimate three different quantities. First, the distance between the satellite and the mean sea surface is used to estimate the ocean surface topography, which yields information regarding a variety of ocean dynamical and geophysical phenomena, for example surface geostrophic currents. Second, sea surface roughness measurements are used to recover estimates of wind speeds, and third, the variability of the sea surface height within the sensor footprint effectively gives an indication of the difference in height between the troughs and crests of ocean waves, thereby allowing estimates of significant wave height. Radar altimeter measurements are virtually independent of cloud cover (Robinson, 2004). For the purposes of this study, the first of the above mentioned measurements is considered, namely the mean dynamic topography of the ocean and its anomaly.

Because of the extreme horizontal thermal gradients and sea level anomalies present in the Agulhas Current region, it is a particularly attractive region to study using satellite remote sensing observations such as those from radiometry and microwave altimetry. Previous analyses of altimeter data for the region have shown a seasonal variation in the inter-ocean exchange via the Agulhas Retroflection (Feron et al., 1992). Furthermore, high and low frequency variability studies have been under taken in the Agulhas Current system using satellite altimeter data (Minster and Gennero (1995) and Wang and Koblinsky (1996)), and more recently, combining satellite altimetry with infra-red images (van Leeuwen et al., 2000), it was shown that the so-called Natal Pulses may play an important role in an Agulhas Ring shedding event. Altimeter data has often been used in conjunction with other satellite observations, such as Sea Surface Temperatures (SST), or in situ data, to confirm the presence of, or distinguish between, meanders and eddies, e.g. Rouault et al. (2006), and these data have been used in research and cruise planning. They provide extensive spatial and temporal coverage of the ocean, and play a vital role in understanding the circulation and its mesoscale variability.

In this initial evaluation of altimetry data for the Agulhas Current region SLA maps, merged from TOPEX/Poseidon, Jason-1 and ERS-1/2 altimeter data, were compared to Jason-1 SLA along-track data to determine the degree of smoothing of information in generating merged maps for the Agulhas Current region. The mapping method used to produce the gridded SLA maps has been outlined in detail by Ducet et al. (2000). The gridded data has a horizontal resolution of $1/3^\circ$ on a Mercator grid, which therefore provides SLA maps with a grid-resolution of 24 km to 37 km in the Agulhas region. These maps are available at weekly intervals.

When examining the flow structure and mesoscale variability of the Agulhas Current system, the data available from the Jason-1 tracks and merged SLA maps is ideal. The tracks from Jason-1 provide very good spatial coverage of the area, and their alignment is virtually perpendicular to the flow of the Agulhas Return Current.

The data were obtained via ftp from the SSALTO/DUACS near-real time and delayed time multi−mission altimeter data processing system under CNES (Centre National d'Etudes Spatiales). The delayed time com-

ponent of the SSALTO/DUACS system utilised in this study has been designed to process data from TOPEX/Poseidon, Jason-1 ERS-1/2, GFO and ENVISAT altimeters to provide a homogenous, inter-calibrated and highly accurate long time series of SLA and merged SLA altimeter data. For more details regarding the delayed- and real-time SLA data products refer to SSALTO/DUACS User Handbook (2004).

3.1 Data processing and analysis

Numerous studies have discussed the mapping capabilities of merging multiple satellite altimeter data, and have shown that combining data from two or three altimetry missions reduces the mapping error significantly (Traon and Dibarboure, 1999). Mapping errors, although not homogenous remain sufficiently small relative to the signal observed. It remains unclear to what extent the information is smoothed from interpolating data from multiple altimeter missions onto a Mercator grid. For the purpose of further variability studies and model validation, along-track data from two tracks will be analysed and compared to calculated monthly mean SLA surface maps, in an attempt to quantify their discrepancy in the Agulhas Current region. SLA data for a two year period, from May 2002 to January 2004 was analysed.

For data processing, reading programs are available for data extraction from CLS (Collecte Localisation Satellites). Following the data extraction, MatLab algorithms were devised which selected the data of a specified track and grouped it according to successive cycles. Overlapping data, which occurred in its raw form, was cut and a general reprocessing of the data into a MatLab matrix format was achieved, allowing for further manipulation and analysis.

3.2 Jason-1 repeat track analysis

The available tracks from Jason-1 (red) in the Agulhas Current system together with ocean bathymetry data (blue) from ETOPO-2 are shown in Figure 2 (left). The depths vary from more than 4000 m, in the Agulhas Basin, to less than 500 m, on the Agulhas Bank. Water depths decrease to around 2000 m at the Agulhas Plateau, centered at approximately 26 °E and 39 °S.

As has been mentioned, the satellite coverage of this region is extensive, with each track being repeated once every 10 days, during which time the satellite orbits the Earth 127 times, this gives a track separation of 317 km at the equator, which is practically identical to the orbit of TOPEX / Poseidon (Robinson, 2004). The descending track alignment is almost perpendicular to the Agulhas Current flow, this presents a very good opportunity for repeat-track analysis of the system with altimetry.

The two Jason-1 tracks (Figure 2; right) selected for the comparative analysis and geostrophic flow calculations were chosen, because of their location close to the Agulhas Plateau, around which high flow variability has been documented in the past. Furthermore, the flow dynamics in the region are dominated by the presence of a semi-permanent geographically trapped meander, which is centered around the Agulhas Plateau.

Hovmoeller plots (Figures 3 and 4) for the two year time period of the two selected tracks were plotted,

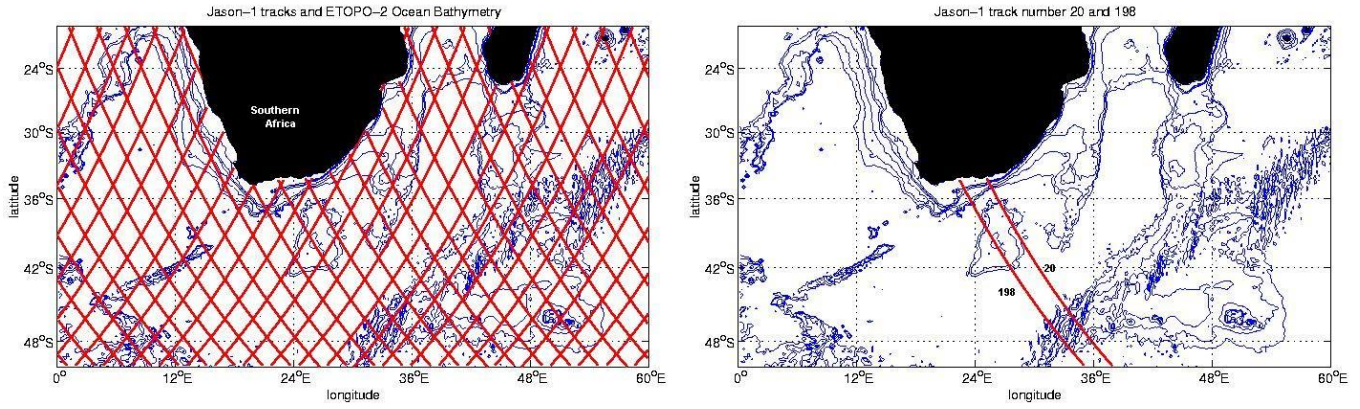

Figure 2: *Jason-1 track paths for the Agulhas region. Left: all available tracks. Right: tracks 198 and 20 selected for the purpose of this study.*

showing SLA in (left; in cm) and corresponding geostrophic currents (right; in m.s^{-1}) perpendicular to the track. The white areas in the Hovmoeller plots represent missing data.

The colour scheme represents the sea surface height in centimeters, for the SLA plots, and the geostrophic current velocity in m.s^{-1}, where red (positive) is indicative of northeastward, and blue (negative) is indicative of southwestward flow anomalies. In all cases, the zero contour is represented by the black line, to be able to distinguish between positive and negative anomalies.

Note that U and V flow components may only be decomposed for crossover points (see Figure 2, left). This was not included in the scope of this study.

Remote sensing of ocean parameters from space have inherent positive advantages in terms of temporal and spatial coverage, as revealed by the Jason-1 tracks (Figure 2). Furthermore, the ability of microwave radiation to penetrate cloud cover effectively, allows for good data coverage in the greater Agulhas Current system, a region of very persistent cloud cover (Quartly and Srokosz, 2002).

The 10-day repeat tracks from Jason-1, represented in the Hovmoeller plots of both SLA and calculated

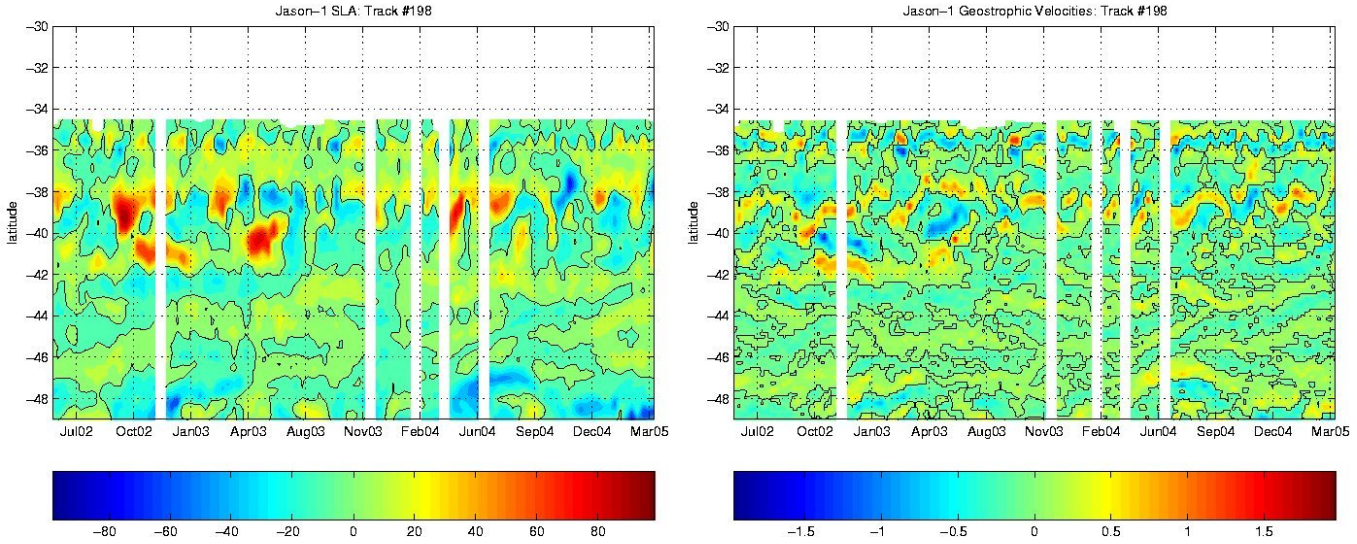

Figure 3: *Hovmoeller plots of Jason-1 track 198. Left: sea level anomaly (SLA; in cm). Right: calculated geostrophic velocities (in* m.s^{-1}*).*

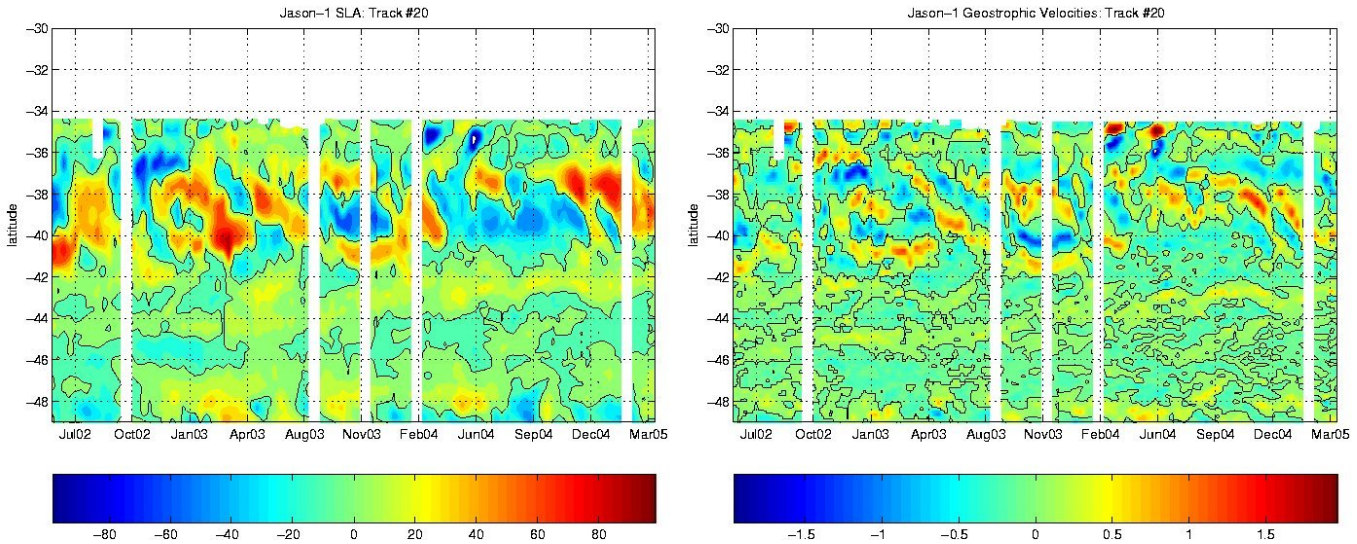

Figure 4: *Hovmoeller plots of Jason-1 track 20. Left: sea level anomaly (SLA; in cm). Right: calculated geostrophic velocities (in* m.s^{-1}*).*

geostrophic velocities (Figures 3 and 4), give a very good indication of the spatial and temporal variability in the Agulhas Current system. In both tracks, most of the strong anomaly features appear to be located north of 42 °S latitude, which correlates well with the previously documented position of the Agulhas Return Current. Evidence of variability in the Agulhas Current proper, in the northern extremes of the figures, does not seem to appear in the SLA, suggesting that the current flow close to the coast is indeed very stable, and does not exhibit much temporal and spatial variability. There are however a few anomaly structures that propagate through the Agulhas Current proper, evident particularly in track 198, where the current flow is forced away from the coast, due to topographic steering by the Agulhas Bank, resulting in shear edge eddies and meanders. However, these features, located around 36 °S (Figure 3), are not nearly as strong as the anomaly features located within the Agulhas Return Current, around 40 °S.

The anomaly features presumably associated with the Agulhas Return Current between 38 °S and 42 °S have very strong gradients, ranging from 80 cm below the mean sea level to more than 80 cm above, giving rise to very strong geostrophic currents, as seen in Figures 3 and 4 (right). Geostrophic currents of up to 2 $m.s^{-1}$ have been calculated, which is consistent with previous velocity estimates in the region (Boebel et al., 2003a). The flow regime seems to exhibit a stronger tendency towards an easterly flow, associated with the Agulhas Return Current, and further south, the South Atlantic Drift or Antarctic Circumpolar Current. A south-facing slope will generate an eastward geostrophic current, whereas a north-facing slope will generate a westward flow. These figures confirm the strong temporal and spatial variability of the system.

The southeastward propagation of the anomalies, both positive and negative, as shown in track 20, seem to be related to the geographically trapped meander flanking the Agulhas Plateau. This suggests a highly variable flow regime in this particular area. The flow variability seems less pronounced in the more westerly track 198 and the distinct southeasterly propagation pattern is not present. This may suggest are comparatively more stable flow.

In both cases, there is striking temporal variability. It would be presumptuous to assume that this variability is seasonal, but there definitely seems to be a bi-annual signal, with the dominance of positive anomalies for some months and then replaced with a predominant negative anomaly for the next few months. One may argue, that strong positive SLA appear mostly in the summer months, whereas negative SLA mostly in the winter months. This may be due to seasonal thermal expansion, and it seems that this trend is evident in Figure 4, although, a longer time series, or a more quantitative statistical method would be required to confirm this. Such a method, a Fourier analysis, is applied in Chapter 6.3.

3.3 Merged SLA monthly averages

Monthly averages calculated from the 7-day merged SLA maps are shown in Figure 5, in an effort to describe the seasonal variability of the system. The colour scheme indicates sea level anomalies (in cm), ranging from 120 cm below to 80 cm above the mean sea level. Jason-1 tracks 20 and 198 have been included as geographical reference for the purpose of comparison.

The monthly averages calculated from the merged SLA maps (Figure 5), further confirm the temporal and spatial variability in this part of the ocean. The strong SLA associated with the Agulhas Current system are evident, especially in respect of the Agulhas Return Current, the Agulhas Retroflection and Eddies occluded from this region can be seen drifting into the South Atlantic Ocean. The Agulhas Current proper signal is less evident, due to the stable current flow resulting in weak anomalies. This is further smoothed from calculating monthly means. There is however evidence of anomaly features propagating southwards in the system.

Looking at successive images, anomaly features, or eddies, south of Madagascar travel westward and flow into the Agulhas Current, but then seem to dissipate. This might be due to their interaction with the strong current flow here, or from a loss of the signal from the mean calculation. Although the signal is weak, there does seem to be a general southwestward flow close to the coast.

The amplitudes of the anomaly structures increase intensely at the Retroflection. Here large eddies seem to be occluded at frequent intervals, between four and six annually, and travel into the South Atlantic Ocean, generally following a northwesterly track. These eddies have diameters, of approximately 200 km or more, dissipating slowly as they move into the Atlantic Ocean, they have a long life-span, one eddy could be followed from 06 °E / 33 °S in December 2002 to 00 °E / 30 °S in October 2003 (Figure 5). It is unclear if the

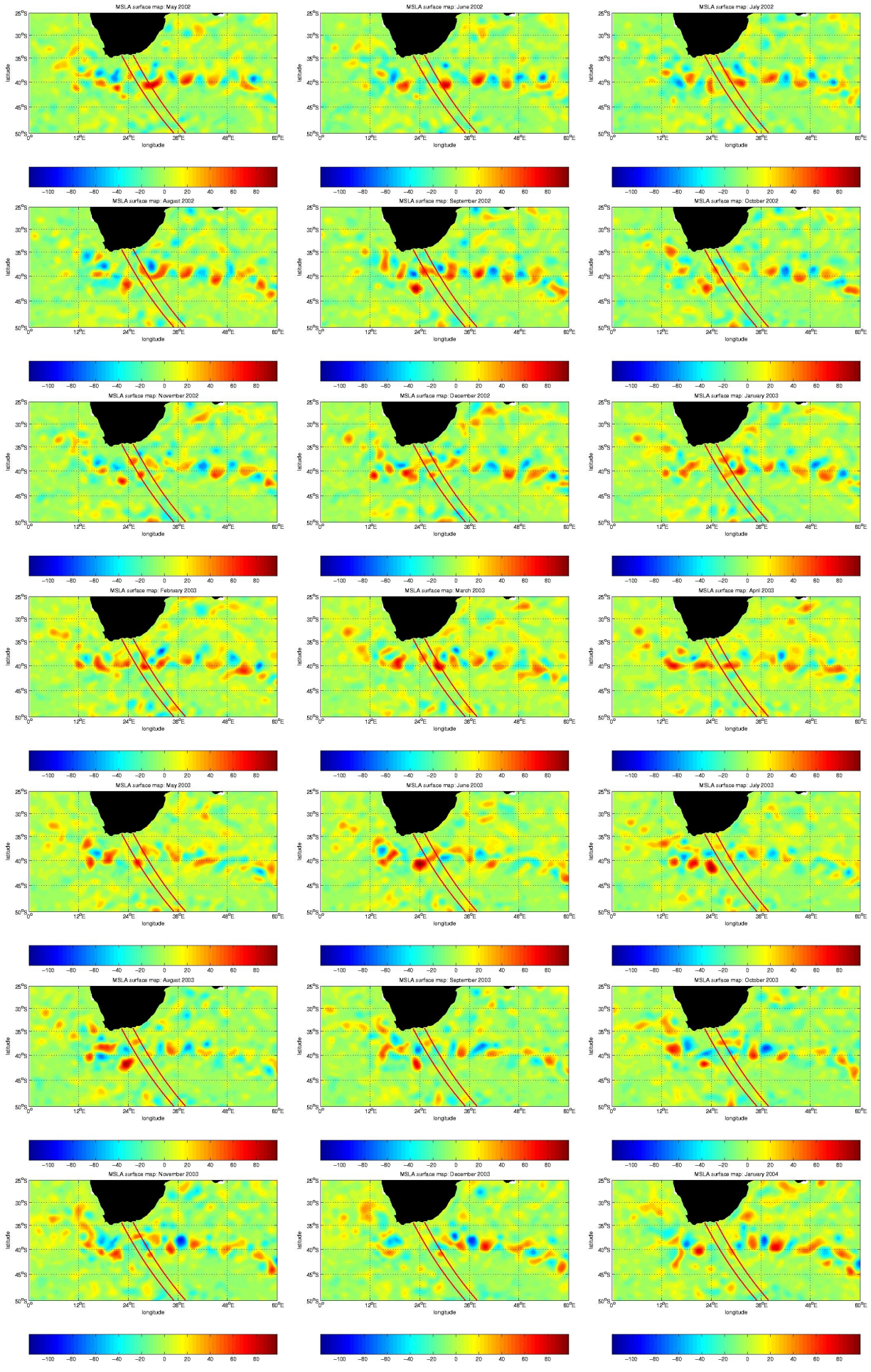

Figure 5: *Merged SLA maps monthly averages (in cm), from June 2002 to January 2004.*

eddy formation is associated with Natal Pulses, it seems rather, that ring occlusion occurs with an eastward migration of the Retroflection Loop and an eventual pinching off of an eddy. The cold core cyclonic Natal Pulses seem to be apparent at times, for example in August 2002 at 25 °E / 35 °S, which coincides with the Jason-1 track 20. Unfortunately the data closer to the coast is missing in this instance, but there seems to be evidence of the negative anomaly in the following cycle.

The Agulhas Return Current exhibits strong mesoscale variability. This is evident throughout the data period. The belt of positive and negative SLA along the 40 °S latitude, reflects the meandering nature of the Agulhas Return Current. The strong anomaly features present here are a result of current meanders rather than of eddies. Towards the eastern extent of the images, the features adopt a progressively more southerly position, which is consistent with reports of the Agulhas Return Current and Agulhas Front, that show a tendency to deviate southwards at higher longitudes (Belkin and Gordon, 1996).

In determining seasonal variability, there seems to be a trend, that during summer months the variability in the system is greater. The anomaly features in the Agulhas Return Current seem to be amplified and occur more frequently. There also seems to be more activity in the northern part of the Agulhas Current system, implying that more energy is introduced into the system from the tropics through summer heating. These features seem to be absent during the winter months, with a reduced amplitude and frequency in the Agulhas Return Current meanders, and less activity in the northern regions. These are however observational assumptions from only two years of data and are not supported by statistical analyses.

When comparing the SLA maps with the along-track Jason-1 SLA Hovmoeller plots, one can see that they are very well correlated. It seems that the geographical position and amplitude of the anomaly features apparent in the merged SLA data compares well with the repeat track data. This suggests that the anomaly signal remains intact when providing the 7-day merged SLA maps, and furthermore there is no significant loss, or smoothing, of the data when calculating monthly means.

In terms of uses for SLA data in operational oceanography, the data is ideal for model validation and data assimilations. The Agulhas Current system is fairly stable, so that most large scale changes are represented in the SLA maps available every 7 days. Furthermore, the data provides a good supporting tool for oceanographic surveys of anomaly features, in respect of tracking and positioning and hence in advancing the understanding on ocean interior variability and flow regimes of the Agulhas Current system.

3.4 Summary

Satellite Altimetry is well adapted for open ocean SLA analysis. Both the gridded map and along-track data describe the Agulhas Current system flow regime and its mesoscale variability well. The two data are well correlated, suggesting that there is no significant loss, or smoothing of information from producing the 7-day merged maps, and calculating monthly means from these.

The calculated geostrophic currents from the along-track SLA data, displays velocities of up to 2 $\mathrm{m.s^{-1}}$ in agreement with reported results (Boebel et al., 2003a), with a predominant easterly flow component, and associated variability from anomaly features propagating through the system.

There is however a problem in using these data for topographically stable currents. In such a case the sea surface height becomes smoothed out in the mean when calculating SLA. The implication is that geostrophic current estimates will be too low. This is evidently the case for the Agulhas Current and some of the stationary meanders in the Agulhas Return Current.

The fact that the mean SLA maps and along-track data correlate well has positive implications for operational uses of this data product. The relatively stable conditions observed in the Agulhas Current system, therefore suggest that the merged SLA maps, integrated over 7 days provide a very good spatial picture of the flow regime. This situation of relatively slow moving variability and good representation thereof in gridded SLA maps has very practical applications for assimilation of such data in numerical ocean models. Since it allows for an update of the model using time-synchronous data and does not require assumptions to be made regarding the time-decorrelation. Furthermore, in model validation and process studies, this will allow us to extract data from the merged SLA maps along favourable sections for propagation and variability analyses (Chapter 6.3), without fearing a significant loss of information from smoothing, providing a strong support tool in model validation.

4 Model characteristics and setup

4.1 The Hybrid Coordinate Ocean Model (HYCOM)

Developed from the Miami Isopycnic Coordinate Ocean Model (MICOM; Bleck and Smith (1990)), HYCOM is a primitive equation model, which combines the best features of isopycnic-coordinate and fixed-grid ocean circulation models within one framework (Bleck, 2002). Simulating oceanic circulation, isopycnic vertical coordinates in ocean models have the advantage of retaining water mass properties over long time integrations. However, these models were not designed to represent unstratified or convectively unstable water columns. HYCOM is able to avoid the problems which might occur in simulating such water columns by smoothly interchanging the vertical coordinates between isopycnic, in the stratified open ocean, z-level coordinates, for resolving the upper-ocean mixed layer dynamic processes, and σ-coordinates, which follow the bathymetry, in shallow coastal regions.

Based on work by Holland et al. (1998) and Webb et al. (1998), Winther et al. (2005) implemented a fourth order numerical momentum advection scheme in HYCOM, and evaluated it in terms of its efficiency compared to the classical second order scheme. They have shown that the fourth order advection scheme reduces the minimum number of grid cells required to accurately represent an oceanic feature (e.g. an eddy), from eight grid cells, in the second order scheme, to four grid cells. Furthermore the fourth order scheme yields more realistic results without increasing the grid resolution and has improved conservation of potential vorticity properties. Thus at length scales similar to the deformation radius the fourth order numerical scheme for momentum advection is more cost effective than doubling the resolution. The higher order advection scheme (QUICK-scheme; B.P.Leonard (1979)) was not implemented in this study, but it is cited here as a possible source for improving the simulations of the region.

4.1.1 Vertical coordinate scheme

Simulating the vertical movement of water masses in ocean models can be divided into two forms of representation: Lagrangian and Eulerian motion. Representation as Lagrangian motion, as in isopycnic models, allows the coordinate surface to move with the respective water masses in the vertical. Thereby retaining water mass characteristics over long time periods. The Eulerian approach, used in z-level and σ-coordinate models, utilises a fixed vertical coordinate system, where water is allowed to pass through a coordinate surface.

The principal difference of HYCOM from other numerical ocean models is that it uses both methods of representation, this can be best described in the definition of the equation of continuity:

$$\frac{\partial}{\partial t_s}(\frac{\partial p}{\partial s}) + \nabla_s \cdot (\mathbf{v}\frac{\partial p}{\partial s}) + \frac{\partial}{\partial s}(\dot{s}\frac{\partial p}{\partial s}) = 0 \tag{1}$$

where $\mathbf{v} = (u, v)$ is the horizontal velocity vector, p the pressure and s the vertical coordinate. The vertical mass flux through a surface (s) is described by the term $\dot{s}\partial p/\partial s$, which is the fundamental term in hybrid coordinate modelling. It determines the spacing and movement of the layer interfaces, termed the "grid generator".

All layers have an assigned reference density. Furthermore, a minimum layer thickness is defined for all layers except for the deep layers intersecting the ocean topography. This allows the vertical coordinate layers to maintain a finite thickness, by switching from isopycnic coordinates to z-level coordinates when the upper isopycnic layer approaches this minimum thickness. During these vertical coordinate interchanges, emphasis is placed on restoring the grid to isopycnic coordinates.

4.1.2 Mixing processes

The horizontal advection and mixing of layer thickness, tracers and momentum is achieved in HYCOM, similarly to MICOM, by using a two-dimensional calculation acting on individual layers. The horizontal advection of layer thickness results in a vertical movement of the layer interfaces, and horizontal diffusion of temperature and salinity in the isopycnic layers may lead to a deviation from the reference density. This may result in two water masses, of the the same density but different temperatures or salinities, to form

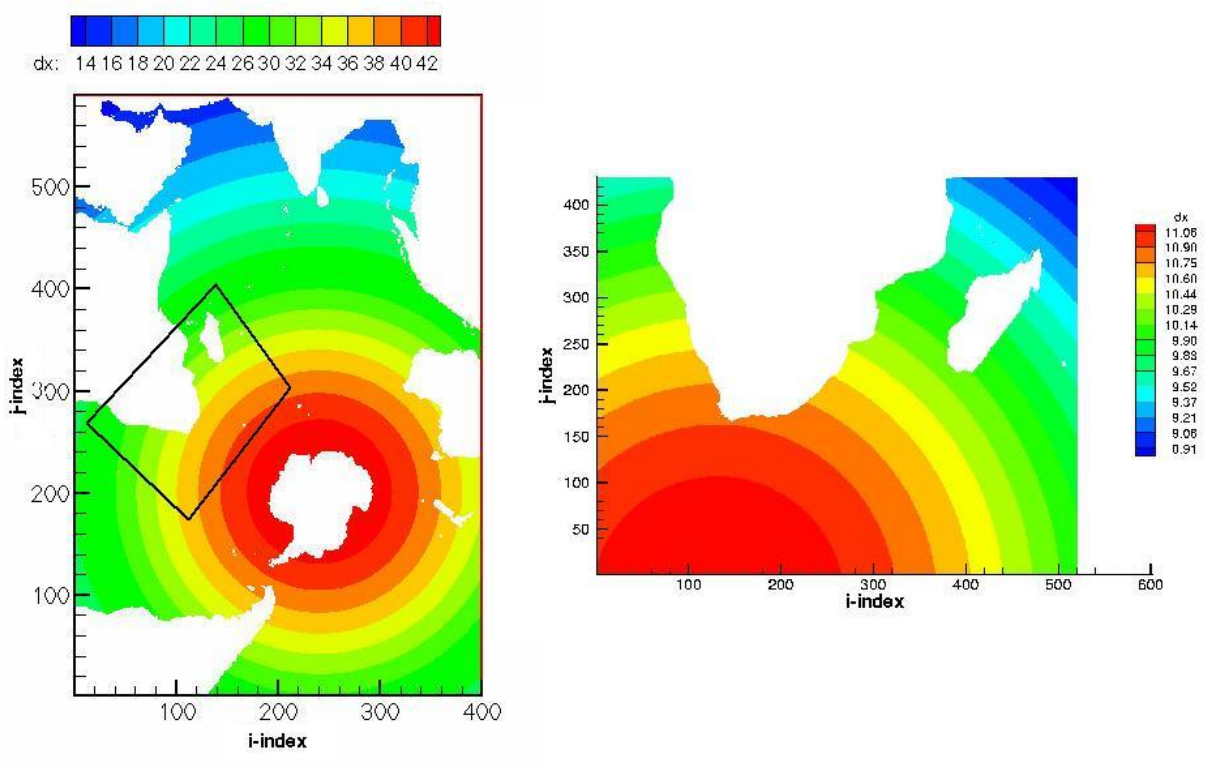

Figure 6: *The HYCOM model system. Left: the basin-scale model of Indian and Southern Ocean (INDIA). Right: the regional model of the greater Agulhas Current system (AGULHAS). The colour scheme indicates their respective grid resolutions in kilometers.*

a new water mass with a different density. To avoid this, the "grid generator" is required to restore the coordinate surface to their reference densities at each time step.

Vertical mixing is simulated through a combination of cabbeling, restoration processes and explicitly prescribed physical mixing. The vertical mixing scheme employed in the NERSC-version of HYCOM is the K-Profile Parameterization (KPP; Large et al. (1994)). It mixes the entire water column by matching surface boundary layer mixing parameterization to that of the ocean interior, and takes into account mixing processes resulting from wind and mixed layer turbulence. Additional mixing parameterization for internal wave breaking, vertical current shear, salt fingering and double diffusion processes are defined, and a background vertical mixing coefficient ensures diapycnal diffusion in the deep ocean.

An examination of HYCOM simulations in the shelf sea region of the North Sea (Winther and Evensen, 2006) suggested the use of an enhanced KPP mixing scheme to reduce erroneous mixing on shallow continental shelves. Additionally it was shown, that the KPP mixing scheme is sensitive to the presence of freshwater, which implies that an improved representation of freshwater input is required, instead of the monthly mean climatology presently used.

4.2 Model setup

The HYCOM system set up to simulate the greater Agulhas Current region involves two models: a coarse resolution, basin-scale model of the Indian and Southern Oceans (INDIA), and a nested, regional model for the Agulhas Current system (AGULHAS; Figure 6).

4.2.1 Nesting procedures

In the NERSC-version of HYCOM we use a one way nesting scheme, where boundary conditions for AGULHAS are relaxed towards the output provided by the coarser INDIA model. For the slow varying variables such as baroclinic velocity, temperature, salinity and layer interfaces, the boundary condition calculations are based on the flow relaxation scheme (FRS; Davies (1983)). The barotropic variables are treated in a hyperbolic wave equation for pressure and vertically integrated velocities (Browning and Kreiss (1982) and

Browning and Kreiss (1986)), these must be treated carefully to avoid reflection of waves at the open model boundaries. Numerical instabilities do occur at the boundary, and it is important that these do not affect the region of study.

The INDIA model dumps values for the regional AGULHAS model boundaries, interpolated to the higher resolution grid, every 6 hours. The regional model then reads the boundary conditions every 6 hours, and interpolates in time for the individual time steps. Neither of the models include tides.

4.2.2 Basin-scale Indian Ocean HYCOM

The basin-scale model INDIA, which provides boundary conditions for the regional model of the Agulhas Current has been set up at the Mohn-Sverdrup Center (courtesy of Belma B. Batlak). Its horizontal resolution ranges from 14 to 40 km with 30 vertical layers. Around Southern Africa and the Agulhas Current the resolution range is between 30 and 40 km, which is insufficient to resolve the mesoscale variability occurring in this region. The model bathymetry was interpolated from GEBCO (General Bathymetric Chart of the Oceans; www.ngdc.noaa.gov/mgg/gebco) at 1' resolution. INDIA was initialised from the Generalized Digital Environmental Model (GDEM; Teague et al. (1990)) data, and an 8 year spin-up period was run with monthly climatology forcing fields.

Following which a simulation experiment was run from January 1992 to December 2004. And INDIA provided boundary conditions for the AGULHAS HYCOM from January 2000 onwards. Forcing fields for the model were obtained from a combination of data: COADS (Comprehensive Ocean-Atmosphere Data Set; Slutz et al. (1985)) provided cloud cover data, precipitation data was obtained from Legates and Willmott (1990) and synoptic atmospheric forcing fields from ECMWF (European Centre for Medium−Range Weather Forecasts). Note that all atmospheric forcing fields have a horizontal grid resolution of $0.5\,^{\circ}$. River influx has been modelled as a negative salinity flux, and the major rivers in the Indian Ocean basin have been added, including the Zambezi River on the East African Coast.

4.2.3 Regional Agulhas Current HYCOM

The regional model was set up to include the Agulhas Current proper, the Agulhas Retroflection and the Agulhas Return Current, such that their dynamics are unaffected by inaccuracies which may arise at the boundaries. The resulting geographical grid extends from approximately $0\,^{\circ}$ to $60\,^{\circ}$ east and from $10\,^{\circ}$ to $50\,^{\circ}$ south, with a horizontal resolution between 8 and 11 km (Figure 6), which has been deemed sufficient to resolve the mesoscale variability of the system.

The vertical discretization in the model uses 30 hybrid layers, with target densities, referenced to σ_0 ($= 1000\ kg.m^{-3}$), ranging from 21.0 to 28.3. These were chosen to be the same as in the INDIA HYCOM to avoid potential problems when interpolating between layers at the boundary. Forcing fields are the same as for the basin-scale model, with the exception that no river fluxes were included. The model grids have been created using the conformal mapping tools developed by Bentsen et al. (1999). AGULHAS was initialised from INDIA HYCOM data fields interpolated onto the high resolution grid, and a simulation experiment was run from January 2000 to December 2004, with a spin-up period of approximately four months from January to April 2000.

Note that at this grid size and resolution, the CPU usage for one week integration of AGULHAS corresponded to 3.5 CPU hours on 8 processors, i.e. 5 years of model integration corresponded to approximately 40 CPU days (barring any problems).

5 General circulation from the model velocity fields

An analysis of the velocity fields from the Agulhas HYCOM reveals that the general circulation features in the greater Agulhas Current system are well described in the first three years of the simulation (Figure 7; left). The latter two years see the development of an anormal anticyclonic circulation feature, which adversely affects the downstream circulation (Figure 7; right). The development of this feature will be discussed in later chapters.

In both the mean surface velocities (Figure 7), and the weekly average surface velocities (Figure 8), we see evidence of the East Madagascar Current (EMC), which splits into its northern and southern branches near 17 °S, as described in previous literature (Lutjeharms et al., 2000). Surface velocities in the southern

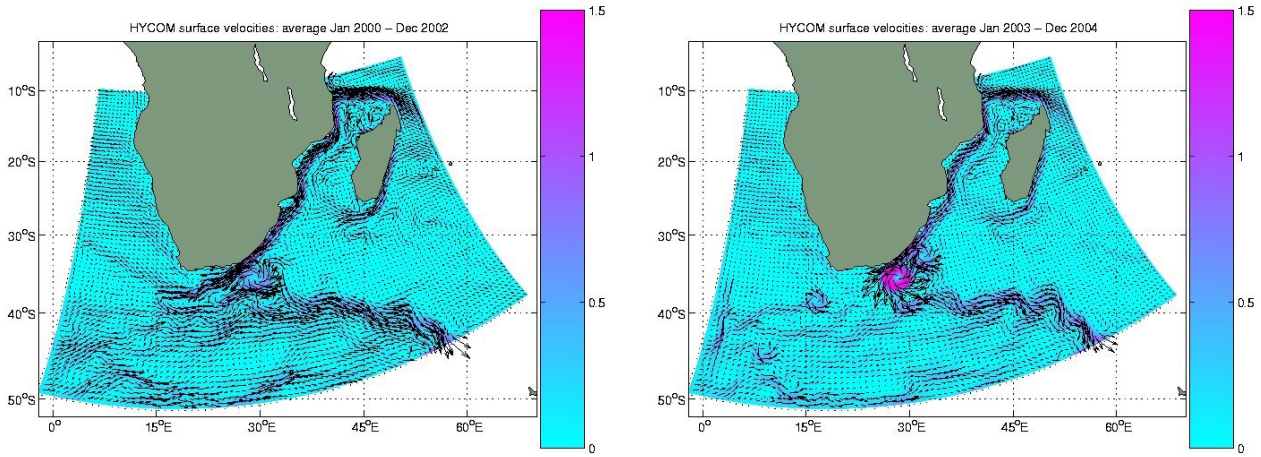

Figure 7: *Average surface velocity ($m.s^{-1}$) fields from HYCOM. Left: average from combined years 2000, 2001 and 2002. Right: average from combined years 2003 and 2004.*

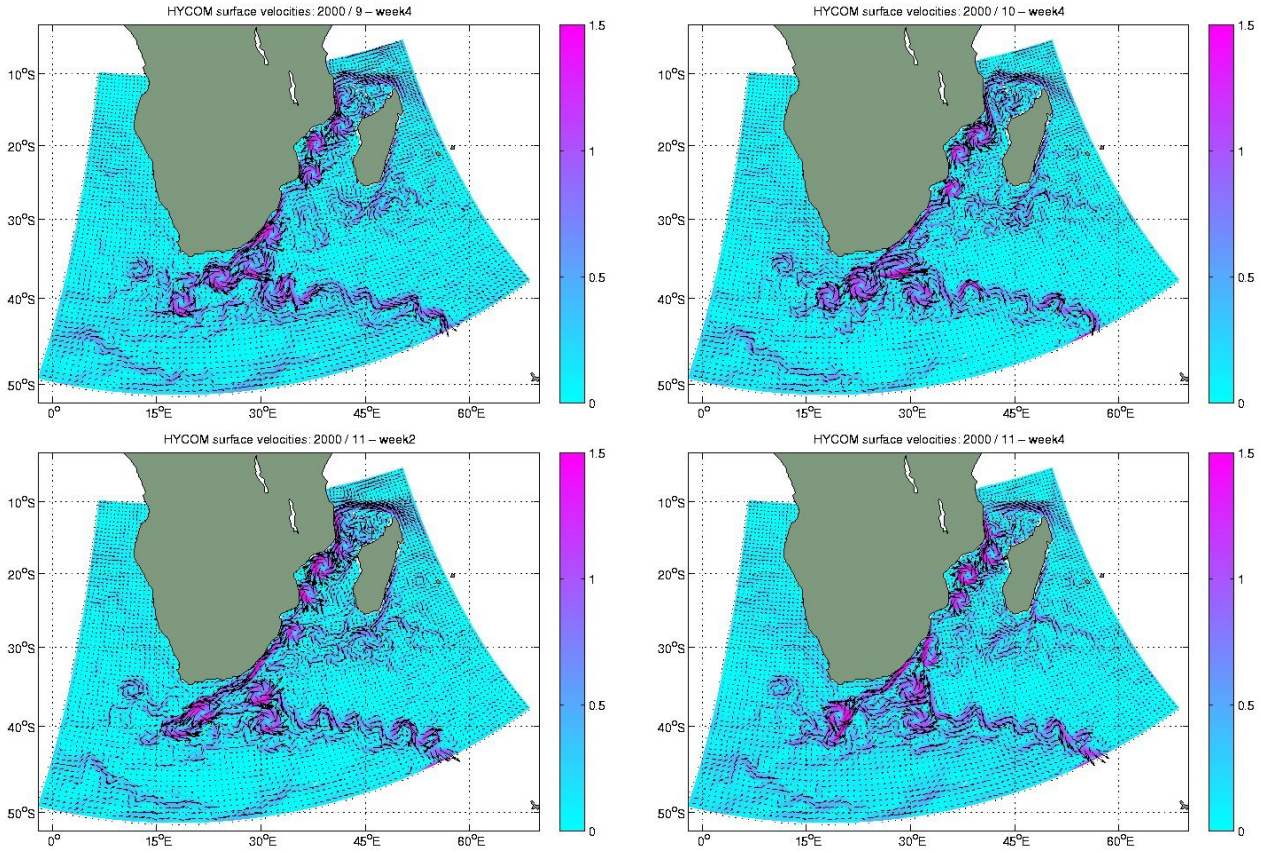

Figure 8: *Weekly surface velocity ($m.s^{-1}$) fields from HYCOM.*

branch reach up to 0.7 m.s^{-1}, with stronger velocities evident off the northern tip of Madagascar.

With the termination of the Madagascar Island to the south, the EMC forms an anticyclonic Retroflection loop, similar to the Agulhas Current Retroflection. The weekly data from HYCOM reveals eddies occluding from the Retroflection, which travel west toward the African continent, and eventually join the Agulhas Current.

Referring to Figure 7, the main features of the Agulhas Current, with the exception of the anticyclonic recirculation centered around 35 °S and 30 °E, are well represented in the model. In the north, the Agulhas Current proper intensifies near 27 °S and closely follows the shelf edge, which here lies close to the coast, consistent with observations to date. Surface velocities exceeding 1.5 m.s^{-1} can be seen near the coast at its fully constituted state between 30 °S and 35 °S.

The flow through the Mozambique Channel is dominated by southward progressing eddies. This is not evident in the mean flow field but is very apparent in the weekly data. Their analysis revealed that these eddies tend to form north of the Davies Ridge, near 15 °S, and then move southward, keeping to the western edge of the channel, eventually connecting with the Agulhas Current proper (Figure 8). This provides the basis for our assumption in Chapter 6.3, where their progression is more thoroughly discussed in relation to sea level anomalies.

With a widening of the continental shelf near 35 °S, the current is seen to depart from the coast. The weekly data (Figure 8) here show the current to meander and numerous eddies can be seen associated with its path variability.

Following the current departure from the coast, it continues on its southwesterly meandering path eventually retroflecting in an anticyclonic loop near 16 °E. The position of the current Retroflection displays strong temporal and spatial variability (Figure 8). The dynamics in these southern reaches seem very chaotic, with the presence of large anticyclonic circulation features seemingly dominating the flow regime. It might be surmised that the large anormal recirculation feature, which diverts the Agulhas Current core in an early Retroflection later on in the simulation, can already be seen to develop late in the year 2000.

At the Agulhas Retroflection, numerous eddies have been seen to be shed, drifting into the South Atlantic Ocean following a northwesterly path.

The core of the remainder of the current, flows eastward between 39 °S and 40 °S toward the South Indian Ocean, in what is known as the Agulhas Return Current. This return current is known to display strong mesoscale variability in its flow. Semi-permanent meanders are evident in the mean velocity field at approximately the positions described in previous literature. Its flow at higher latitudes towards the east is also evident.

With the development of an anormal circulation feature upstream in the in the Agulhas Current proper, the downstream circulation and mesoscale variability associated with the southern Agulhas Current disappears. Most of the flow is diverted eastward and very little flow circulation is evident in the southern regions. The development of this feature will be discussed in later chapters, it is clear however, that this feature is not apparent in the observations, and is most likely associated to model inaccuaries.

6 Model validation

Model validation is an exhaustive task, and requires many inter-comparisons with observational data. Recent developments in satellite remote sensing and altimetry have been instrumental in supplying data where, in the Agulhas Current region to date, there has been a general paucity of observations available. They provide a powerful means for model validation, at least for the upper ocean.

Our focus here is the use of satellite altimetry in model validation for the greater Agulhas Current system. Detailed validation of the INDIA HYCOM is presently being undertaken at the Mohn-Sverdrup Center (M-SC.). We touch on the work achieved in the INDIA HYCOM validation so far in the context of its importance with respect to providing boundary conditions for the high resolution nested AGULHAS HYCOM. An investigation into the thermal-haline vertical structure of the regional model is important in terms of explaining some of the phenomenon evident. To this end available hydrographic data from the

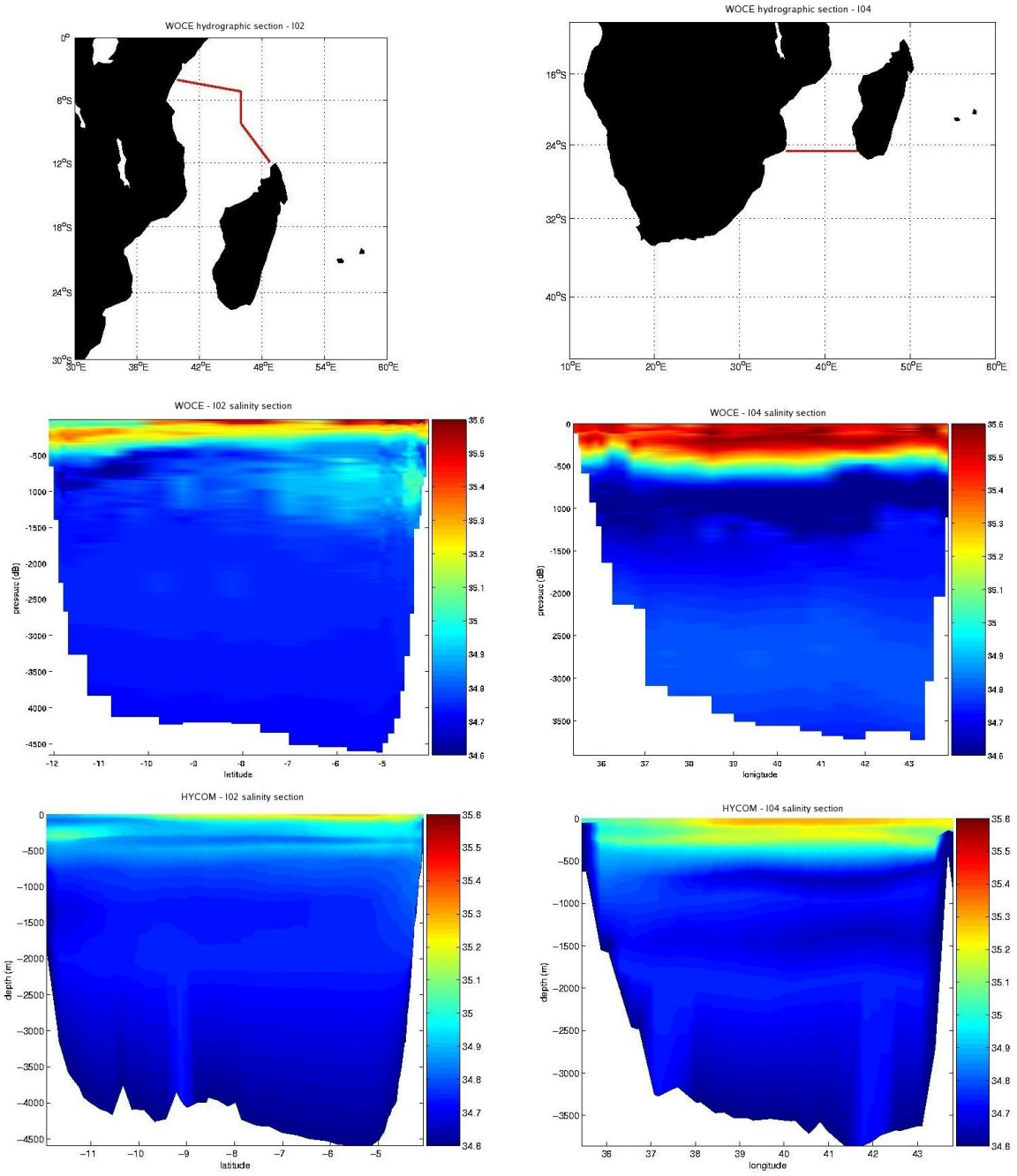

Figure 9: *Comparison of salinity data from the WOCE hydrographic programme in 1995, (middle figures), to sections from INDIA HYCOM (bottom figures). Left column: WOCE section I02. Right column: WOCE section I04.*

GoodHope programme was used.

Preliminary validation of the INDIA model (Batlak, 2005) suggests that the model is able to reproduce the general circulation, the water masses and volume transports for selected regions. This is confirmed by additional validation (Ms. Swapna George and Mr. Rahman Mankettikkara; M-SC., 2005), who have shown that the model is able to represent the major surface current circulation patterns in the Indian Ocean, and the respective current velocities conform with published results.

Further comparisons to available hydrographic data from the World Ocean Experiment (WOCE, cruise data 1995; Figure 9) show that there is a salinity deficit of up to 0.3 psu in the upper 500 m, in the source region of the Agulhas Current during that period.

A general salinity deficit in the parent model has inherent negative implications when providing boundary conditions for the nested regional model. Too fresh waters would lead to a lack of baroclinicity, with too weak vertical stratification in the model. This would favour the barotropic instabilities and emphasise the larger features. This may result in the formation of excessively large eddies.

Upon further investigation (Batlak, 2005), salinity deficits were observed in the equatorial regions, and this problem may be associated with the model initialization from-, and relaxation to-, GDEM. Comparisons of GDEM climatology to a 10-year mean field from the model shows that salinities near the Agulhas Current do not vary significantly from the climatology (pers. comm. Ms. Swapna George, M-SC.).

More recent ARGO float profiles for the region near the Agulhas Current show comparable values for the model simulation, giving us relative confidence in the boundary conditions supplied for the nested Agulhas Current model. The source of the salinity deficit in our model simulations remains unresolved.

6.1 Comparison to GoodHope II: salinity section

The GoodHope programme aims at establishing regular observations across the Southern Ocean between Africa and the Antarctic (Ansorge et al., 2005), where to date observational data has been sparse.

From the comparison (Figure 10), it is clearly evident that our model simulation lacks the required salinity gradient of the region, and as described previously this has inherent negative implications in simulating ocean dynamics. It seems likely that the salinity deficit in the AGULHAS HYCOM has been inherited from the parent model providing boundary conditions which are too fresh (Figure 9).

The general structure is poorly represented in the model. The more saline Agulhas Current waters evident between 34 °S and 38 °S displays a salinity deficit of almost 0.6 psu in the model. Fresher Antarctic Surface waters can be seen in the southern reaches of the section, and subduction associated with the Subtropical Convergence (STC) and Subantarctic Front (SAF) can been seen to occur near 44 °S in both the observations and the model simulation. Again the gradients are too weak and not comparable.

From the hydrographic data, it seems evident that there is an advection of saline waters from the Agulhas Current into the South Atlantic Ocean. The model discrepancy to the observations may be related to the anormal circulation feature which has developed by this time, causing an early Retroflection of the current and a general decrease in the mesoscale variability usually associated with this region. This feature may not allow the usually saline Agulhas Current waters to reach this region, accounting for the decreased salinity gradient evident here.

6.2 Comparison to TMI-AMSR satellite SST

The use of microwave remote sensing has the advantage of being virtually unaffected by cloud cover. In the region of the Agulhas Current, where extensive cloud cover has been known to persist over long periods of time (Lutjeharms et al., 1986) this has distinct advantages.

Sea surface temperatures (SST) optimally interpolated from two microwave imagers are used here, the Tropical Rainfall Measuring Mission (TRMM) Microwave Imager (TMI), and the Advanced Microwave Scanning Radiometer (AMSR-E) onboard NASA's Aqua satellite. The period from June 2002 to July 2004 was readily available from a previous study (Rouault et al., 2006), and is utilised here as a climatological means of model validation and description of its general features.

Optimal interpolation of the two data results in daily near-global coverage of the ocean surface temperature, with a horizontal grid resolution of ∼25 km. Figure 11 shows the mean SST (in °C) of the region from TMI-AMSR and from HYCOM. In HYCOM the averages were divided into two periods, January

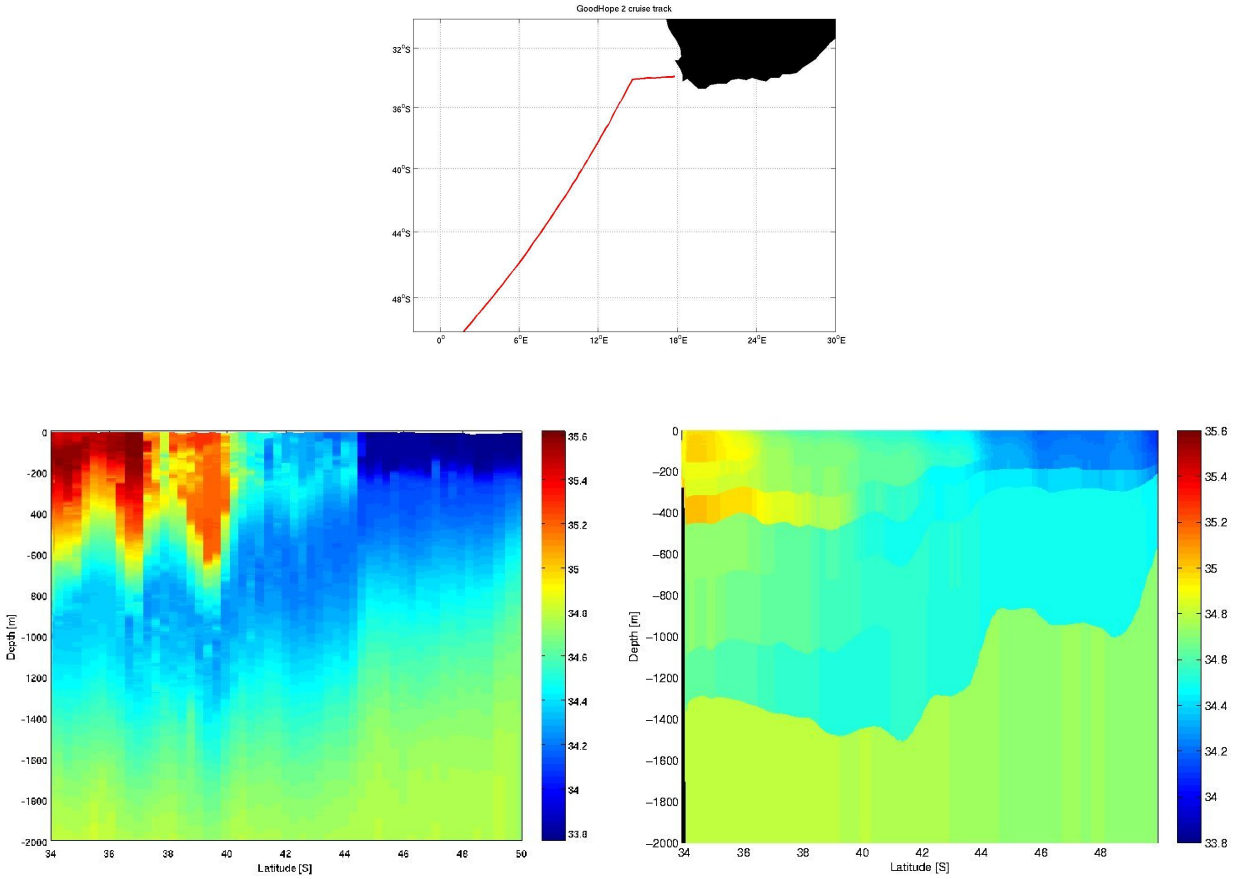

Figure 10: *Comparison of salinity data from the GoodHope programme in November 2004, data made available by Dr. Sergey Gladyshev (P.P. Shirshov Institute of Oceanology of the Russian Academy of Sciences). Left: GoodHope II salinity section. Right: AGULHAS HYCOM salinity section.*

2000 to December 2002 and January 2003 to December 2004. The latter describing the period following the development of the anormal cirulation feature. The isotherms 20 ° and 22 ° were selected to represent the extent of the Agulhas Current, with 17.9 °, 14.2 ° and 7 ° the respective frontal zones associated with the Antarctic Circumpolar Current (ACC), as determined by Lutjeharms and Valentine (1984). The 14.2 ° isotherm represents the surface expression of the Subtropical Convergence (STC), and 17.9 ° indicating its northern most extent.

The effect of the anticyclonic feature can be clearly seen (Figure 11; right). Both averages from HYCOM lack the southwestward penetration of the Agulhas Current, evident in the TMI-AMSR SST. The anormal circulation which seemingly develops over time may be held accountable for this. As a consequence, our model simulation does not yield sufficient advection of warm Agulhas Current water into the South Atlantic Ocean. This can be seen from the 17.9 ° isotherm southeast of Cape Town. Here it is narrower than the observations in the first three years, and separated from the South Atlantic Ocean in the last two years.

The first three years seem to be able to represent the semi-permanent meanders in the Agulhas Return Current. However they are not as pronounced, and disappear entirely with the development of the early Retroflection in the latter two years. The mean position of the of STC, represented by the 14.2 ° isotherm, is relatively well represented in the model simulation.

HYCOM is also able to represent the Benguela Upwelling System along the west coast of South Africa. Barring the extent of the Agulhas Current, the general surface water temperatures seem well represented, with slightly too warm SST's just south of the Mozambique Channel.

It should be remembered that these are very generalised comparisons, where readily available data was used to give some indication of the characteristic SST's of the region. It is important to note the adverse effect the anormal circulation has on the extent of the Agulhas Current, and the associated advection into the South Atlantic. Furthermore for a first run of HYCOM for this region, without data assimilation, many

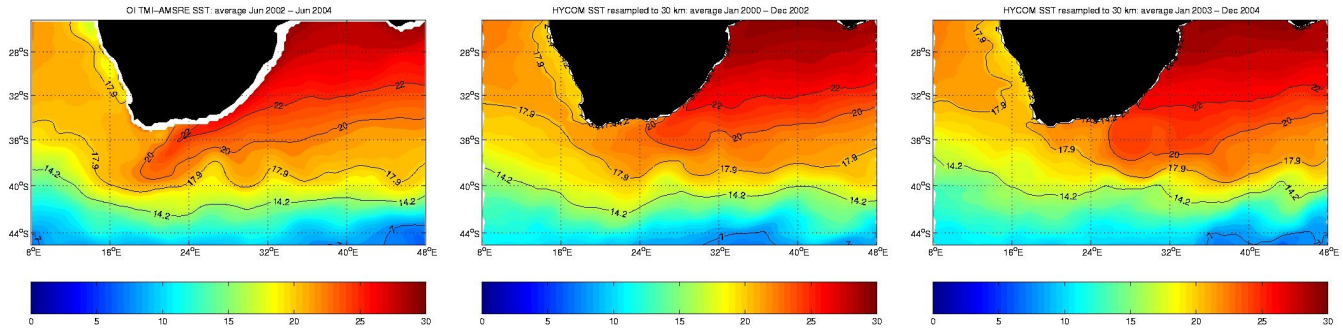

Figure 11: *Mean sea surface temperatures (SST). Left: Optimally interpolated from TRMM and AMSR-E Microwave Imager, from June 2002 to June 2004. Middle: HYCOM SST from January 2000 to December 2002, resampled to a 30 km grid. Right: HYCOM SST from January 2003 to December 2004, resampled to a 30 km grid.*

differences and inaccuracies can be expected. However, in the following variability analyses, it will be shown that the model simulation supports many of our findings, and sheds light on the dominant processes in the upstream region of the Agulhas Current system.

6.3 Comparison to SLA from radar altimetry

In Chapter 3 it was shown that the merged SLA maps provide a good temporal and spatial picture of the flow regime in the Agulhas Current system, and that there seemed to be no significant loss or smoothing of information from the merging of data from multiple altimeter missions to produce the gridded SLA maps. Furthermore, comparisons of calculated monthly mean fields to the along-track data suggests that the Agulhas Current system mesoscale variability is relatively slow moving, such that its temporal and spatial variability can be adequately resolved by the respective altimeter repeat cycles, their ground spacings and the merging of their data.

Following this, data was selected along favourable tracks (Figure 12) for model validation and variability analysis. Data from the 7 day merged altimetry fields was extracted along selected sections and weekly average data from the same sections was extracted from HYCOM for the hindcast simulation period (Figures 13, 14, 15 and 16). These were selected in an attempt to describe the most important features of the Agulhas Current system. Namely, the Agulhas Current proper and Retroflection (Section 1), the Agulhas Retroflection and Return Current (Section 2), and the eddy shedding corridor, where Agulhas Rings have been observed to drift into the South Atlantic Ocean, represented by the western part of Section 2 and Sections 3 and 4. This approach was adopted from Schouten et al. (2002) to include model validation and support in the variability analysis.

From these sections the number of eddies were counted, to intuitively determine statistical comparisons between the altimeter observations and the HYCOM simulation. The frequency and propagation velocity estimates are summarised in Tables 1 and 2.

This process of counting eddies is a very subjective method of determining comparative statistics for model simulations from observations. The focus here is tracking positive SLA features in an attempt to relate the upstream mesoscale variability with the variability observed at the Retroflection. The assumption is that these features represent anticyclonic eddies formed in the Mozambique Channel, which propagate southwestwards and integrate with the off-shore edge of the Agulhas Current. Eventually reaching the Retroflection, where some of these eddies seem to detach themselves and move into the South Atlantic Ocean as Agulhas Rings. This assumption is confirmed, to a degree of certainty, by comparisons to the mapped SLA data (e.g. Figure 5) and are strongly supported by the weekly average surface velocity fields of our model (Figure 8). To estimate anticyclonic eddy frequencies in each of the four sections, each was sub-divided into a set of sub-regions (Table 1).

Eddy frequencies were determined for the entire data period and annual averages were calculated from these. In HYCOM, annual frequency estimates were calculated from three and five year periods to indicate that the first three years of the simulation were considered to be superior to the latter two. For example in Section 2, near 20 °E, all seven eddies observed during the five year simulation experiment were observed

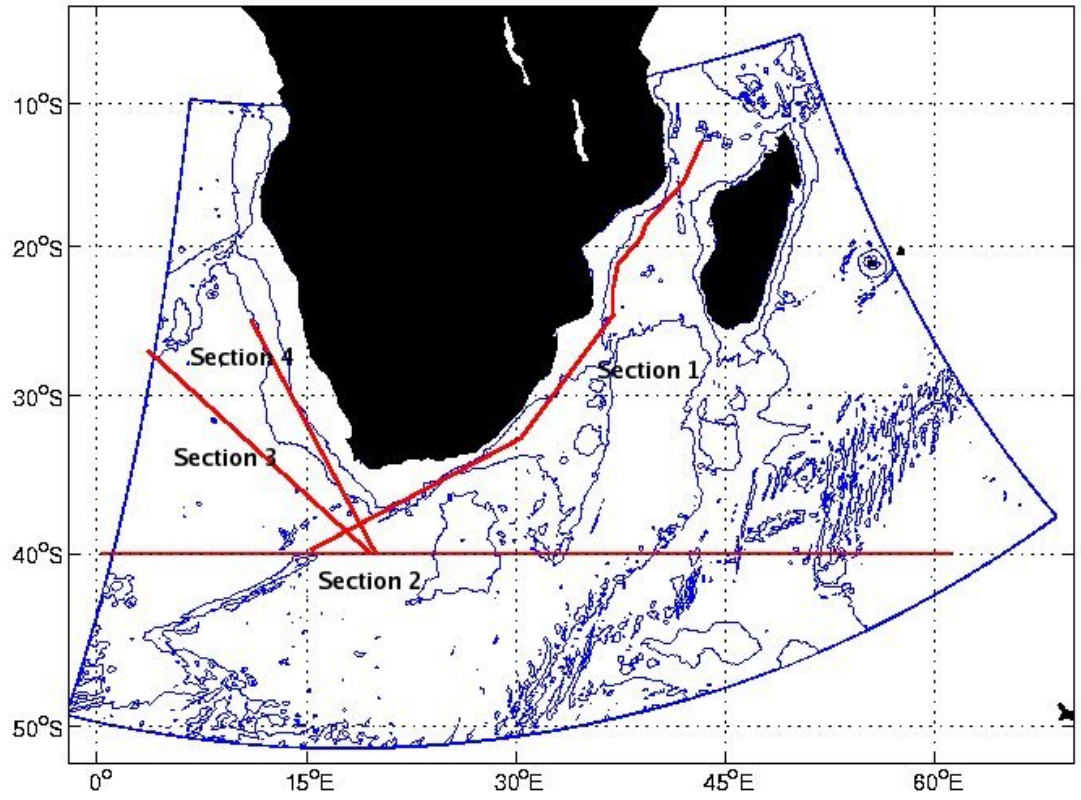

Figure 12: *Map of sections extracted from merged SLA fields and HYCOM, with model grid and bathymetry.*

during the first three years. Similarly in the Agulhas Current (Section 1), south of 35 °S, the variability associated with the current departure from the coast almost vanishes in the years following October 2002. This is thought to be associated with the development of a permanent, large anticyclonic feature upstream of the Agulhas Plateau, in the Agulhas Current proper, causing a early Retroflection of the current (discussed in Chapter 7).

Assuming that the simulation in HYCOM deteriorates in the 4^{th} and 5^{th} years, the annual eddy frequencies estimated from the three year period compare better to the altimeter observations, except in the northern Agulhas, where the annual average from the five year mean is more accurate. The individual sections will be discussed in detail in relation to their respective Fourier analyses.

From the individual eddies observed, propagation velocities were estimated by calculating the distances of each of the sub-regions in the sections, and considering the respective travelling times of each of the anomaly features tracked (Table 2).

Propagation velocity estimates and their standard deviations are given in kilometers per day for all four sections and their sub-regions. Additionally in Section 1, the calculated propagation velocities from the distance along the section "as the crow flies" and "along section points", were included to highlight that the section is not a straight line.

The comparisons to the model vary in the different sections. This is possibly due to the different variability modes of the Agulhas Current system. In the Mozambique Channel and northern (upper) Agulhas Current, HYCOM slightly over-estimates the propagation velocities, the difference however is not very large, and the associated standard deviations from HYCOM suggests variable eddy propagation velocities, which, compared to the altimetry observations, are quite encouraging. Furthermore our estimates of the eddy propagation velocities in the Mozambique Channel compare well with the estimate of 5 km.d^{-1} by Schouten et al. (2002).

It is unclear whether the negative SLA features present near 30 °S in both the altimetry and model data are from the passage of the so-called Natal Pulses (Lutjeharms and Roberts, 1988). These large meanders form approximately 6 times per year at the Natal Bight and move downstream with velocities of approximately 10 km.d^{-1}. They sometimes reach sizes of up to 300 km and are thought to play a role in

		Altimetry observations		HYCOM simulation		
		5 year period	Annual average	5 year period	5 year annual average	3 year annual average
Section 1	Total number observed	20	4	28	5 – 6	9 – 10
	Number observed in Mozambique Channel	18	3 – 4	26	5 – 6	8 – 9
	Number observed in Retroflection region	16	3 – 4	10	2	3 – 4
	Number observed in Retroflection region with origin in Mozambique Channel	14	2 – 3	10	2	3 – 4
Section 2	Total number observed near 20 E	26	5 – 6	7*	1 – 2	2 – 3
	Number observed between 15 – 10 E (shed from Retroflection)	20	4	7	1 – 2	2 – 3
	Number observed between 10 – 0 E (W. Eddy Corridor)	13	2 – 3	5	1	1 – 2
	Number observed between 10 – 0 E (W. Eddy Corridor) originating near 25 E (Agulhas Plateau)	6	1 – 2	4	0 – 1	1 – 2
Section 3	Total number observed (at 18 E - Retroflection)	17	3 – 4	11	2 – 3	3 – 4
	Number observed at 13 E	13	2 – 3	6	1 – 2	2
	Number observed at 10 E	10	2	5	1	2 – 3
	Number observed at 8 E	8	1 – 2	5	1	2 – 3
Section 4	Total number observed (at 19 E – Retroflection)	19	3 – 4	11	2 – 3	3 – 4
	Number observed at 18 E	9	2 – 3	8	1 – 2	2 – 3
	Number observed at 17 E	4	0 – 1	7	1 – 2	2 – 3
	Number observed at 16 E	4	0 – 1	5	1	1 – 2

Table 1: *Frequency estimates of positive SLA features (anticyclonic eddies) in all four sections.*

the formation of Agulhas Rings. Their propagation velocity compares well with our estimates for the positive SLA features in this region, which gives us confidence in the validity of the method applied to calculate the estimates, and the passage of a positive SLA feature is followed by the presence of a negative anomaly.

In the southern (lower) Agulhas Current the comparisons are not as promising. The model underestimates the velocities here by almost 4 km.d^{-1}. The current variability in this region is far more pronounced than in the northern part, exhibiting numerous meanders and shear edge eddies (Lutjeharms et al., 1989), which may account for the model deviation. Eddy propagation estimates from our sections decrease in the southern Agulhas Current. This is due to the afore mentioned increased flow variability, and our extracted sections do not represent the eddy track. The resultant velocity decrease is also captured in the model, suggesting that it also exhibits increased flow variability in this region. This is also supported in the weekly velocity fields from the model. Another source regarding the model underestimate here, may be associated

				Altimetry observations		HYCOM simulation	
			section distances	average velocity (km/day)	standard deviation	average velocity (km/day)	standard deviation
Section 1	Mozambique Channel (15 – 25 S)	as the crow flies	1137 km	6.17	2.27	7.23	1.80
		along section pts.	1191 km	6.47	2.38	7.58	1.89
	Agulhas Current (25 – 35 S) - upper	as the crow flies	1567 km	10.94	3.18	12.27	2.88
		along section pts.	1587 km	11.08	3.22	12.43	2.92
	Agulhas Current (35 – 40 S) - lower	as the crow flies	1047 km	8.78	2.12	5.09	1.63
		along section pts.	1047 km	8.78	2.12	5.09	1.63
Section 2	Agulhas Return Current (25 – 20 E)		426 km	6.23	1.36	4.54	1.57
	Retroflection region (20 – 15 E)		426 km	6.41	2.03	3.75	1.66
	W. Eddy Corridor (15 – 10 E)		426 km	6.14	2.49	3.29	1.09
Section 3	WNW. Eddy Corridor (18 – 13 E)		589 km	4.19	0.76	4.09	1.45
	WNW. Eddy Corridor (13 – 10 E)		349 km	4.40	1.54	3.10	0.81
	WNW. Eddy Corridor (10 – 8 E)		244 km	3.49	0.73	2.63	0.93
Section 4	NNW. Eddy Corridor (19 – 18 E)		198 km	2.75	0.67	2.36	1.07
	NNW. Eddy Corridor (18 – 17 E)		201 km	1.72	0.70	1.83	0.70
	NNW. Eddy Corridor (17 – 16 E)		205 km	2.56	1.09	2.05	0.31

Table 2: *Propagation velocities of positive SLA features (anticyclonic eddies) estimated in all four sections.*

to the early Retroflection of the current, with the development of the afore mentioned anormal circulation.

In the Agulhas Return Current (Section 2), the model again underestimates the propagation velocities, but the velocity standard deviations seem comparable. Previous estimates of the propagation rate of the Retroflection loop vary between 7 and 15 km.d^{-1} (Olson and Evans, 1986). Our estimates from altimetry fall within this range but do not agree with Schouten et al. (2002), who have described the Agulhas Retroflection to move slowly westward at a speed of 13 km.d^{-1}. Similarly to Schouten et al. (2002), the movement of positive SLA features was tracked, to represent the movement of the Agulhas Retroflection, and estimate its velocity at 6 km.d^{-1}, less than half of their estimate. There are numerous possibilities which may explain this difference. Our zonal section was chosen at 40 °S, versus theirs at 39 °S. Our period of observations was shorter by 2 years, data from January 2000 to December 2004 was analysed, whereas their study encompassed years 1993 to 1999. Furthermore, Schouten et al. (2002) applied a high-pass filter with a 200 day cosine window, suppressing the annual and semi-annual cycles, whereafter they applied 30 day running mean. This combination of bandpass filtering accentuates the three to six annual frequencies. However, in respect of the magnitude of the discrepancies between our estimates, these differences seem unlikely to be the cause. It remains that both velocity estimates are based on subjective definitions of eddies, or in this case movement of the Retroflection, which most likely accounts for the disparity.

Sections 3 and 4 describe the northwest eddy corridor, where eddies, after being shed from the Retroflection, have been known to drift into the South Atlantic Ocean at rates of 5-8 km.d^{-1} (Pichevin et al., 1999). Drift velocities from our sections are slightly underestimated. This can be explained by the fact that the eddy track into the South Atlantic is not along a straight line, which means that the signal of the eddy is intermittently lost in our sections. The propagation estimates in the northern track (Section 4) are even slower, and the eddy signal is quite infrequent, suggesting that eddies tend to favour the more southern path. Model comparisons give realistic drift velocities of the eddies in the South Atlantic Ocean. Although from the Hovmoeller plots it is evident that they strongly favour the southern track, and the ring shedding frequency in HYCOM is too low.

Next, to quantify the frequency statistics described in Table 1, and to gain further insight into the dominant variability modes in the Agulhas Current system, a Fourier transform was applied to the time series at every geographical location of each section in both the model and the altimetry observations. From

these the respective power spectra were calculated. In signal processing the Fourier transform decomposes a signal into its component frequencies and amplitudes, describing the dominant frequency modes and their power at a given location.

This was achieved by applying a fast Fourier transform algorithm to calculate the discrete Fourier transform. For a detailed explanation of the Fourier transform and its applications refer to Bracewell (1999). Prior to calculating the fast Fourier transform, the data had to be conditioned to minimise signal noise and leakage. A linear detrending function was applied, and the outer 10% of the data were smoothed by means of sinusoidal tapering function. The resultant power spectra for the altimetry observations and model simulations are given in Figures 13, 14, 15 and 16.

6.3.1 Agulhas Current

Hovmoeller plots and the associated power spectrum from the altimetry and model data extracted along Section 1 are shown in Figure 13, which was chosen to represent the variability in, or near, the Agulhas Current. It shows that strong positive SLA features, which originate in the northern extremities of the Mozambique Channel propagate southwestwards, seemingly with the Agulhas Current and eventually interact at the Retroflection.

It may be presumptuous to assume that the extracted section is representative of the Agulhas Current proper. Bryden et al. (2005), using a year-long moored array of current meters, determined that offshore edge of the Agulhas Current near 31 °S lies at 203 km. Mostly (almost 80% of the time) the current core is found close to the continental slope, within 31 km of the coast. They observed only 5 days of 267 when the

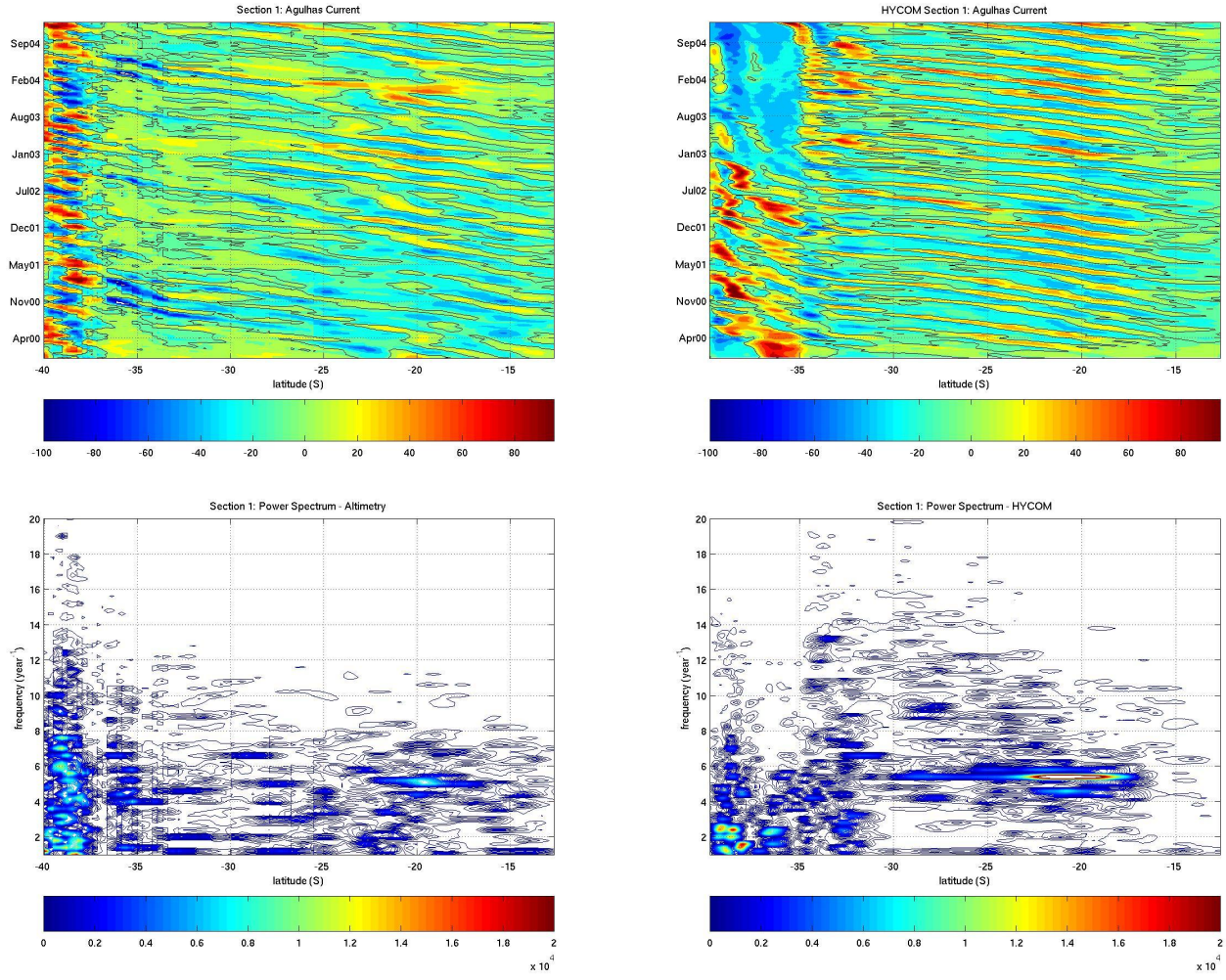

Figure 13: *Section 1, Agulhas Current. Left column: merged SLA altimeter data. Right column: HYCOM SLA data. Top: SLA Hovmoeller plots. Bottom: associated power spectra.*

current was observed offshore at 150 km. It seems likely that the section extracted misses the core of the current, especially between 27 °S and 35 °S where the current is known to follow the continental shelf very closely, with few instabilities, meandering less than 15 km to either side of its path (Gründlingh, 1983). Rather, what is observed represents eddies or meanders in the ocean side of the Agulhas Current.

Nevertheless, there is evidence that the variability evident in the southern Agulhas Current (south of 35 °S), and near the Retroflection, is associated with eddies originating in the Mozambique Channel. This is also strongly supported by our model simulation, which shows that the circulation in the Mozambique Channel is dominated by trains of eddies propagating southwards eventually linking up with the Agulhas Current and the southern regions.

Comparing to the observations, the strength of the variability signal in HYCOM is slightly too high, and a much clearer train of eddies drifting along the Agulhas Current is evident. Conforming with the altimetry observations, increased mesoscale variability is evident south of 35 °S, which is associated to increased current instabilities due to its departure from the coast. Here, growing meanders and shear edge eddies have been observed in the past (Lutjeharms et al., 1989). Unfortunately, the model develops a large, permanent anti-cyclonic feature in October 2002, resulting in an early Retroflection of the current. Furthermore this feature seems to cause the variability associated with the southern Agulhas Current to disappear. The development of this feature will be discussed in more detail in the following chapter.

The power spectra shown are the result of applying the fast Fourier transform to the time series at each point in space. The annual to weekly frequencies are given together with their respective geographical location along the section. In both the model and altimetry observations there seems to be evidence of an annual cycle (1 yr^{-1}) throughout the Agulhas Current. North of 15 °S this may be related to the South Equatorial Current and its association to the monsoonal cycle. Further south this signal may have a variety of sources, e.g. thermal expansion, and is not necessarily driven by the Indian Ocean monsoon, in fact the Agulhas Current is generally thought to be independent of the monsoonal circulation, e.g. Ridderinkhof and de Ruijter (2003). The frequency spectrum in the Agulhas Current is geographically too variable to conclude that clear monsoonal influence exists. Additionally in the more southern regions, between 20 °S and 35 °S, a clear semi-annual (2 yr^{-1}) signal is evident in the altimetry observations, suggesting an additional source of variability. This frequency is however not reflected in the model south of 24 °S, and its source remains unresolved.

A notable feature is the frequency peak of 5 yr^{-1} centered around 20 °S. This very strongly suggests a relation with the passage of eddies in the Mozambique Channel, and is strongly supported by the model simulation. This 5 yr^{-1} peak again appears between 25 °S and 35 °S, with a slight frequency decrease further south. This is expected, since only an intermittent signal is captured in the section with increased current instabilities. The frequency distribution in the model simulation indicates a clear connection of the 5 yr^{-1} frequency in the Mozambique Channel and the southern Agulhas Current.

Near the Agulhas Current proper a range of frequencies is evident, from annual and semi-annual to $\sim$8 yr^{-1} frequencies. This suggests a range of variabilities evident in the Agulhas Current, with no clear dominant mode apparent. The lower frequencies may be explained by seasonal and intra-seasonal signals in the Agulhas Current, e.g. Matano et al. (2001). The frequencies of 5-8 per annum may all be related to eddies, or meanders, propagating downstream with the Agulhas Current.

Closer to the Agulhas Retroflection the signal becomes very unclear, with a suite of frequencies, and there is no distinguishable frequency which stands out above the rest, giving an indication of the unpredictability of the variability in this region. Nevertheless, from the upstream connectivity, it seems reasonable to conclude, that the downstream variability is remotely driven from the upstream occurrences. However, the frequency range and distribution in the south, suggests an additional source of variability.

Comparing these annual frequencies to those given in Table 1, our estimate from altimetry of four per year in the Agulhas Current is relatively accurate, providing additional confidence in the previous propagation velocity estimates (Table 2). Estimates of eddies observed in the Mozambique Channel are slightly too low. The model count compares well with the frequencies described in the power spectrum, especially in the northern Agulhas Current.

From Table 1 it can be estimated that 90% of the eddies observed in the Agulhas Current originate in the Mozambique Channel, and that 78% of these appear to interact at the Retroflection. The model simulation supports this with 93% originating in the Mozambique Channel, but only 38% seem to interact

at the Retroflection. This discrepancy can be accounted for by the development the anormal circulation, as mentioned before. A "best of" percentage calculated from the first 3 years of model integration shows that 64% of the eddies in the Mozambique Channel interact at the Retroflection.

In conclusion, both the subjective and objective statistics, from altimetry observations strongly suggest that the variability in the Agulhas Current and its Retroflection is driven by upstream mechanisms, and that these processes are also related to ring-shedding events. This is strongly supported by the model simulation of the region.

6.3.2 Agulhas Return Current

The Retroflection region, broadly defined between 15 °E and 25 °E, displays active temporal and spatial variability. Previously the variability in this region had been described as non-periodic and discontinuous. Ascribing its variability to ring-shedding events, the formation of Agulhas Rings that drift into the South Atlantic Ocean, with the occlusion of the Retroflection at its western extremity (Lutjeharms and van Ballegooyen, 1988). Schouten et al. (2002) however, show that the Retroflection shows surprisingly regular behaviour, with an east-west oscillating frequency of 4-5 yr^{-1}, and they associated the location of the Retroflection with the arrival of an eddy from the north. Their observations are strongly supported by our observations and model simulation, as described above.

The altimetry observations of the Agulhas Return Current (Figure 14) further support the notion of a regularly east-west oscillating Retroflection, which is further confirmed by a strong 5-7 yr^{-1} frequency near 20 °E in the associated power spectrum. And the upstream connectivity seems to be supported, although it

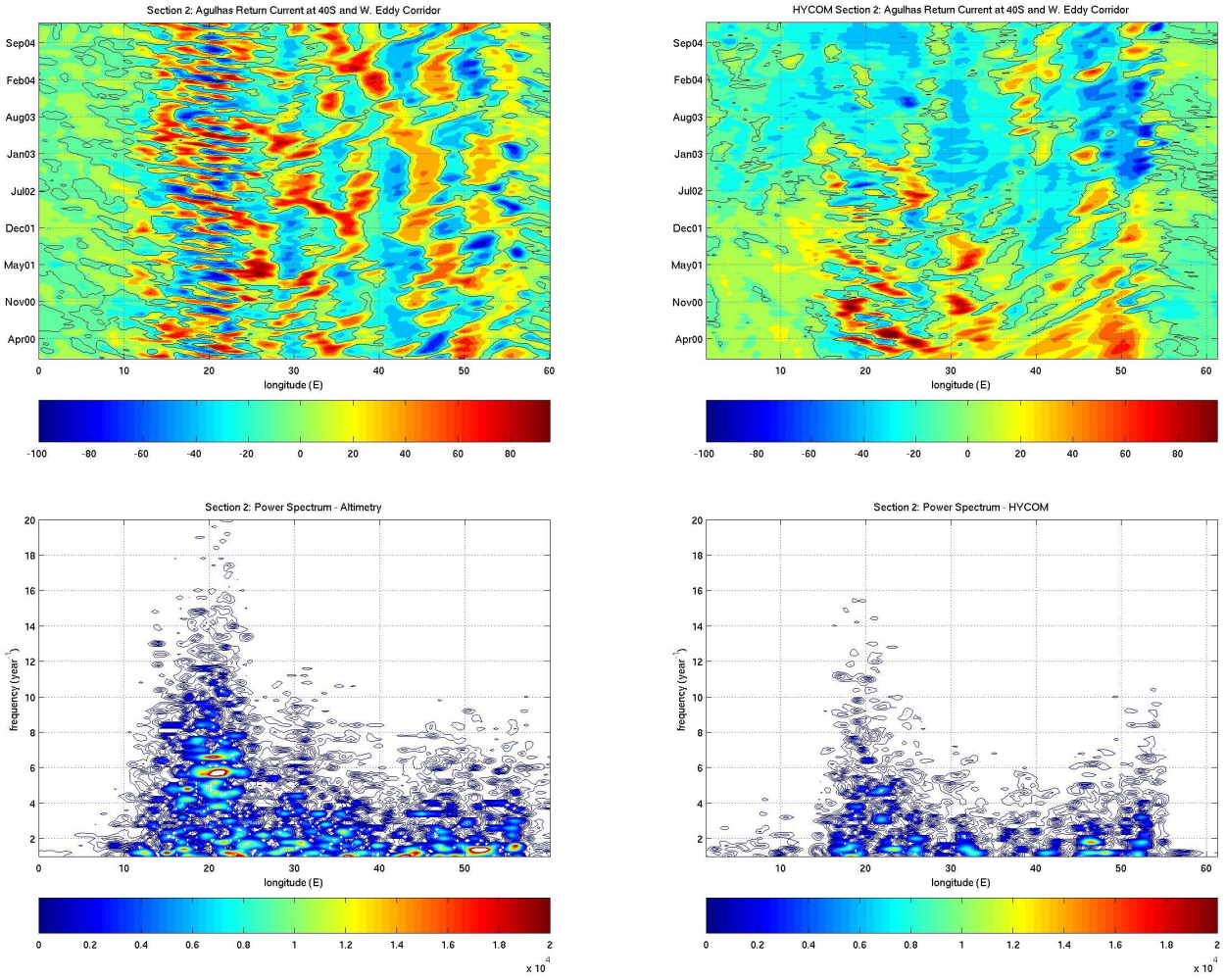

Figure 14: *Section 2, Agulhas Return Current at* 40 °S *and W. Eddy Corridor. Left column: merged SLA altimeter data. Right column: HYCOM SLA data. Top: SLA Hovmoeller plots. Bottom: associated power spectra.*

is difficult to see this connection in the power spectra. The model simulation of this region is not as accurate. However, with respect to the upstream connectivity, there is some confirmation of the Retroflection moving westward with the arrival of an eddy from the northern Agulhas Current prior to the development of the anormal circulation.

Matano et al. (1998) have presented statistical evidence of seasonal variability in SLA of the Agulhas Retroflection region. This seasonal variability occurs in the form of an early Retroflection or bifurcation of the Agulhas Current at approximately 25 °E during the summer months. Our altimetry observations seem to confirm this, with a 1 yr^{-1} frequency peak located near 23 °E in the power spectrum.

Evidence of seasonal variability downstream in the Agulhas Return Current is inconclusive. Contrary to Weeks et al. (1998), Boebel et al. (2003b) detected no clear seasonal pattern regarding the position of the semi-permanent meanders, their southward crests located near 29.7 °E, 35.5 °E and 42.9 °E. Our altimetry observations and associated power spectra disagree with the latter. Seasonal and inter-seasonal variability is evident in the Agulhas Return Current, and there seems to be a relationship with the relative positions of the semi-permanent meanders.

Westward propagating eddies shed from the Retroflection (observed between 10 °E and 15 °E; Table 1) were observed at an average annual frequency of 4 yr^{-1}. An average of 2-3 eddies yr^{-1} were observed westward of 10 °E, with approximately 50% of these are seemingly associated with a westward movement of the Agulhas Retroflection. This presence of eddies in the western eddy corridor is not clearly reflected in the power spectrum. Although one may speculate their presence associated with the frequencies of 1-2 and 3 yr^{-1} at 10 °E.

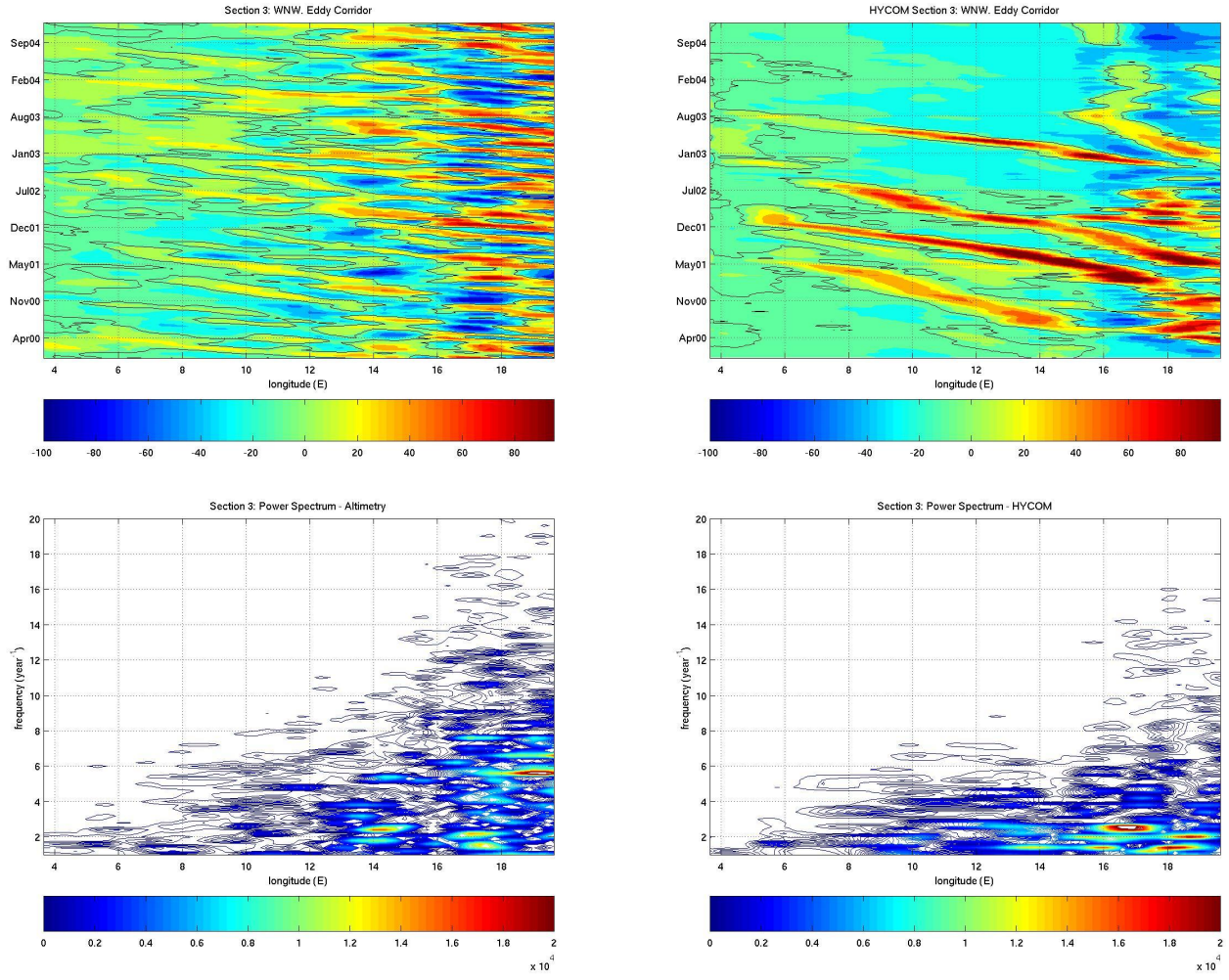

Figure 15: *Section 3, WNW. Eddy Corridor. Left column: merged SLA altimeter data. Right column: HYCOM SLA data. Top: SLA Hovmoeller plots. Bottom: associated power spectra.*

Prior to October 2002, our model simulations suggests an east-west oscillating Retroflection and associated eddy shedding. But following the development of the anormal circulation, HYCOM is not able to accurately represent the variability in the Agulhas Retroflection and the Agulhas Return Current, this is also evident in the respective power spectra.

6.3.3 Eddy shedding corridor

Agulhas Rings are large anticyclonic eddy vortices, which have been observed to drift northwestward into the South Atlantic Ocean at rates of 5-8 km.d^{-1}. These are shed at the westward termination of the Agulhas Retroflection at an average frequency of about 6 yr^{-1} (Pichevin et al., 1999).

From the altimetry observations and model simulations (Figures 15 and 16), it is evident that eddies propagating into the South Atlantic tend to favour the more southerly of the two paths. Intermittent positive SLA signals (Section 3), assumably from eddies, can be observed as far as 6 °E, in accordance with previous literature (Lutjeharms and van Ballegooyen, 1988).

From the power spectra a range of frequencies are evident. The strong signal at 18.5 °E (Section 3) and 19.5 °E (Section 4) are both at about 39 °S and can be related to the east-west oscillating Agulhas Retroflection as described previously. The frequencies of 3-6 yr^{-1}, near 14 °E and 36 °S in Section 3, and 17.6 °E and 36 °S in Section 4, may be associated with Agulhas Ring signals propagating into the South Atlantic Ocean. The distance between these two locations is approximately 330 km, and since eddies of diameters up to 340 km are known to be shed from the Retroflection loop, these frequencies are not necessarily signals from different eddies. Therefore one can only assume that eddies are clearly on the more

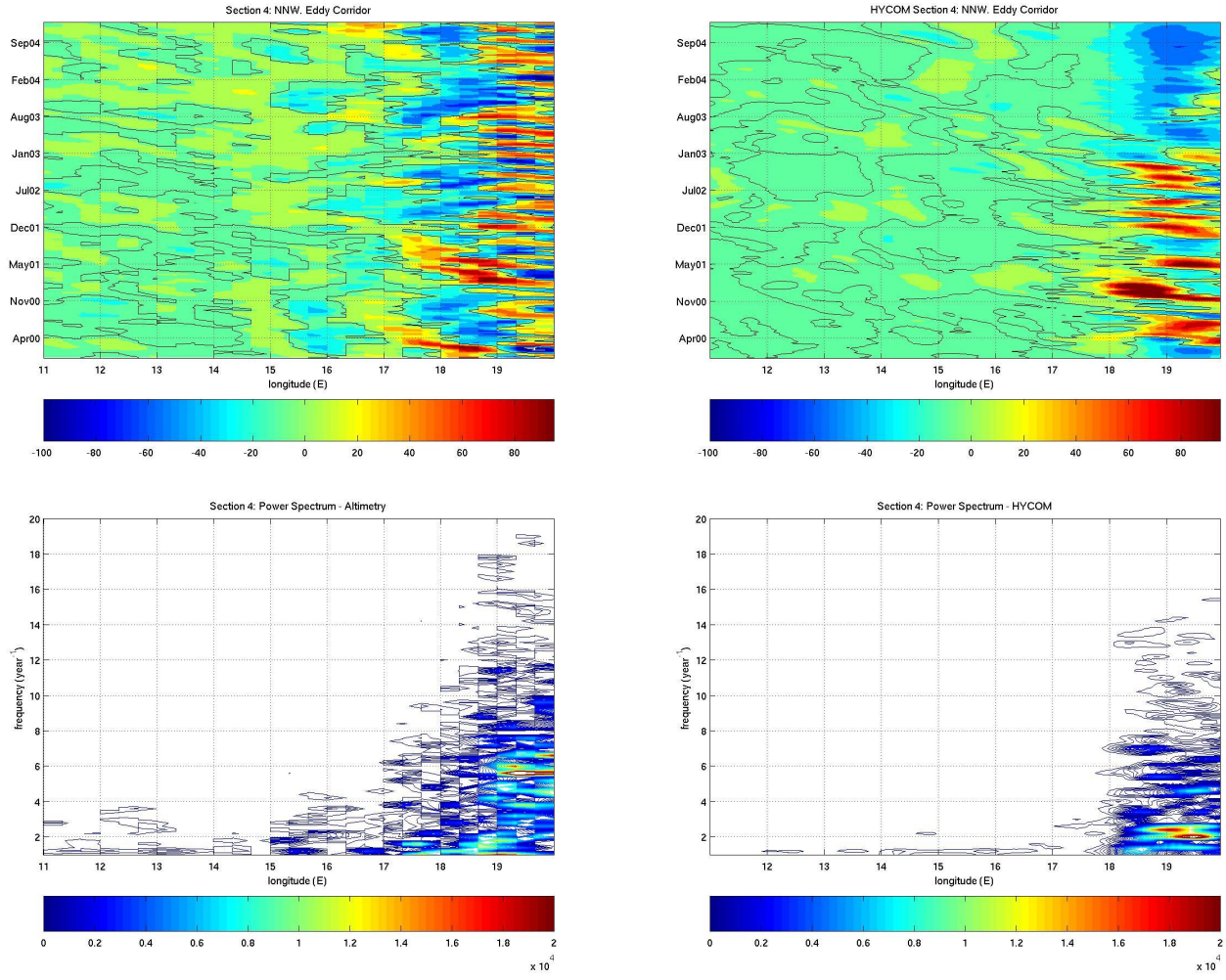

Figure 16: *Section 4, NNW. Eddy Corridor. Left column: merged SLA altimeter data. Right column: HYCOM SLA data. Top: SLA Hovmoeller plots. Bottom: associated power spectra.*

southern path westward of 10 °E. The dominant frequencies near 10 °E range from 2-5 yr^{-1}. Suggesting that eddies following the southern path can be observed between two and five times annually.

Annual and semi-annual signals are also evident in the power spectra. It remains unclear if these are signals associated with the South Atlantic Ocean or Agulhas System seasonality. Especially in the northern path (Section 4) a clear seasonal signal is evident throughout the section, which is unrelated to the track of eddies in this region, but rather to seasonal thermal heating.

Eddy frequency comparisons to Table 1, suggests an underestimate of the number of eddies present in both sections. It remains that the power spectral reading is a statistical means of signal processing, and is perhaps not the ideal method for feature-tracking analyses, where some form of intuitive measure is required. By adding the eddies observed in the respective sections, where one can clearly differentiate between eddies on the west-northwest track, the north-northwest track and the westward track, we estimate an eddy frequency of 5-6 yr^{-1}. This number is to a degree supported by the respective power spectra and in good agreement with previous literature.

7 Eddy Kinetic Energy

The merging of multi-mission altimeter data allows for more realistic sea level and geostrophic velocity statistics than from single altimeters. Furthermore, eddy kinetic energy estimates from the merged product are 30% higher than estimates from TOPEX/Poseidon alone due to increased coverage. It is expected that most ocean eddy energy is conserved in the production of the gridded maps, giving a more accurate description of the ocean circulation, while retaining the accuracy of the TOPEX/Poseidon data but increasing the temporal and spatial resolution. The data has been shown to be in good agreement with in-situ observations (Ducet et al., 2000).

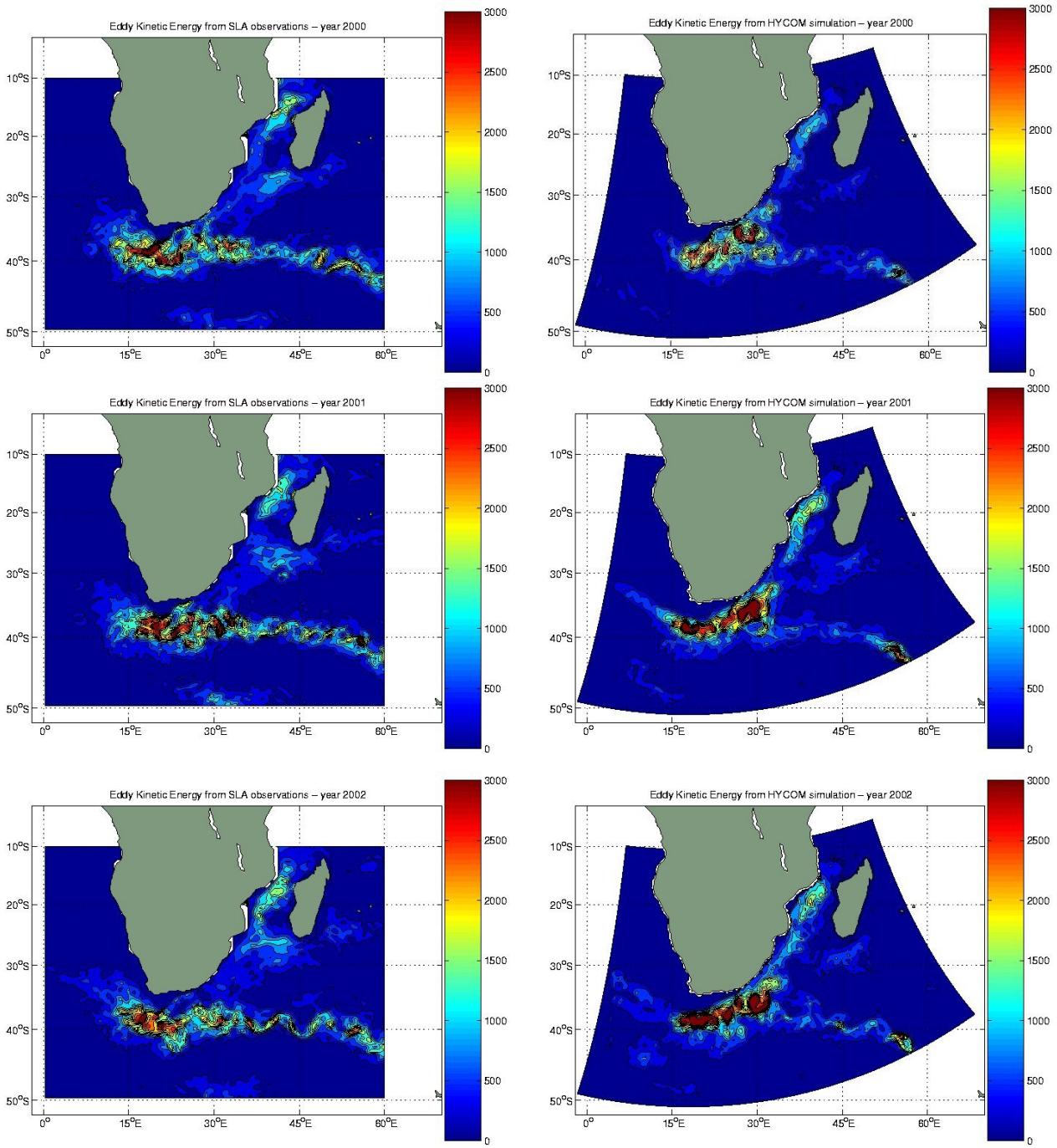

Figure 17: *Annual average eddy kinetic energies (years 2000, 2001 and 2002) for the greater Agulhas Current system. Left: calculated from SLA observations. Right: from HYCOM simulation, resampled to a 30 km grid.*

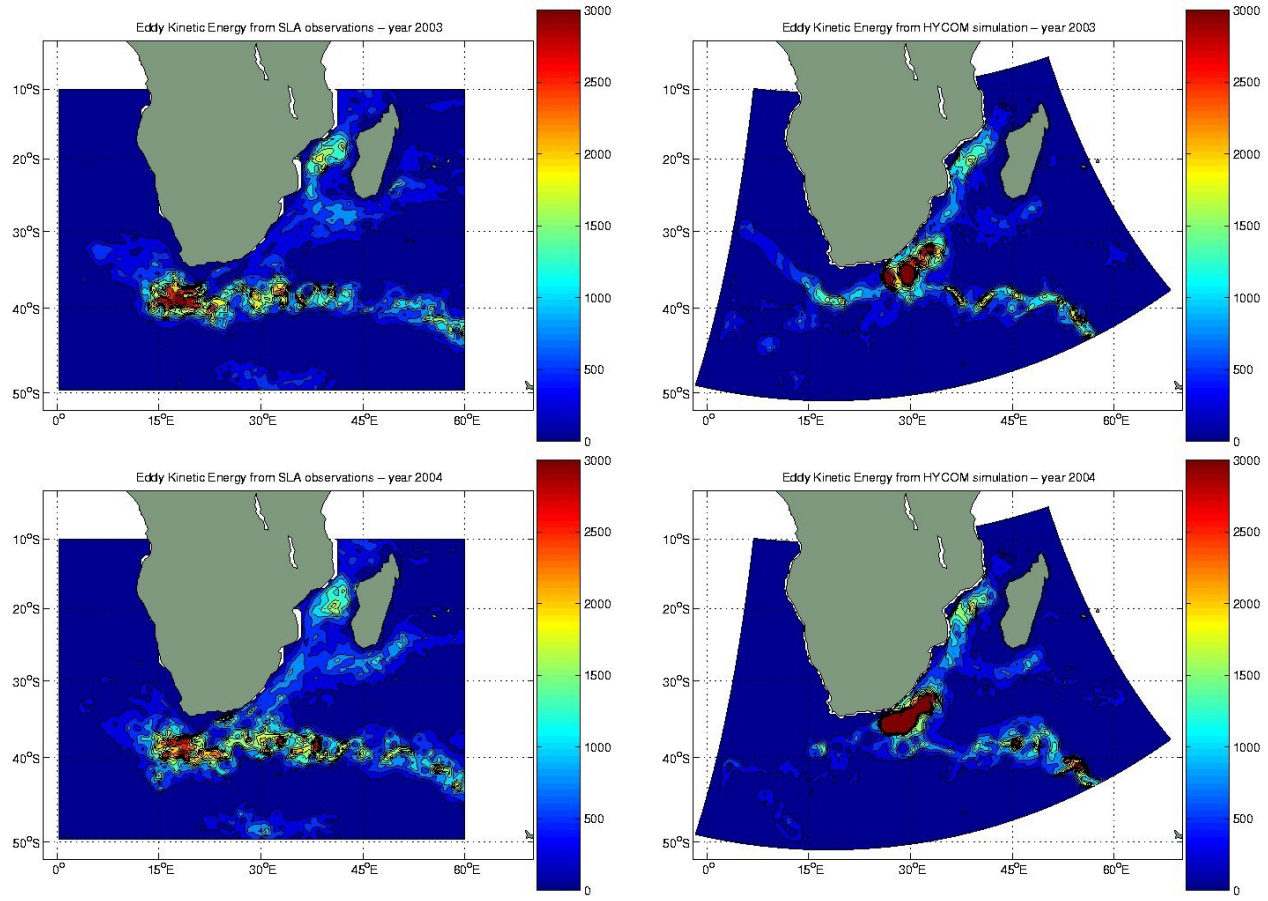

Figure 18: *Annual average eddy kinetic energies (years 2003 and 2004) for the greater Agulhas Current system. Left: calculated from SLA observations. Right: from HYCOM simulation, resampled to a 30 km grid.*

Eddy kinetic energy (EKE) for the greater Agulhas Current system, calculated from altimetry and model fields, is shown for successive years in Figures 17 and 18. They are given in unit of $cm^2.s^{-2}$ and describe the eddy energy distribution in the region. To ensure the comparison of similar wavelengths, HYCOM was resampled to a horizontal grid resolution of 30 km to match the grid projection of the merged SLA product. Weekly averages from HYCOM were used, such that the temporal mean calculation of the two data is comparable. Note that EKE for the model simulation was calculated from the HYCOM SLA fields, to conform with the estimates from SLA observed at the ocean surface.

7.1 Distribution in the greater Agulhas Current system

The Agulhas Current has been documented as one of the most energetic regions in the world, especially in the region of the Agulhas Retroflection and its Return Current (see e.g. Figures 17 and 18). Changes in eddy energy may indirectly result from external forcing, e.g. wind and/or buoyancy effects, these effects however may only play a significant role in areas with low eddy variability, which is not the case for the Agulhas Current system.

In terms of model validation eddy kinetic energy fields are a very beneficial tool, because it allows for a temporal and spatial description of the ocean energy and good comparative means for model simulations.

Yearly average eddy kinetic energies are described in each of the figures and the general features of the greater Agulhas Current system seem to be relatively well described in the model simulation.

Throughout the Mozambique Channel regions of active EKE are displayed, giving further confirmation of the notion that the circulation here is dominated by a succession of eddies propagating downstream and linking up with the Agulhas Current proper, as discussed in the previous chapter.

In both the model and the altimetry data, there seems to be a further link between eddies from the East Madagascar Current (EMC) and the Agulhas Current. An analysis of the velocity fields in HYCOM

reveals that this connection is simulated as eddies shed from a retroflecting EMC, similarly to Agulhas Rings and cyclones shed from the Agulhas Retroflection. These eddies propagate westward towards South Africa, eventually linking up with the Agulhas Current.

EKE in the northern Agulhas Current is less pronounced than the southern regions, this is expected, since topographically stable currents are known to barely be represented in EKE maps (Ducet et al., 2000). This occurs due to a smoothing of the SLA signal in the calculation of a mean sea surface height field,and is also represented in the HYCOM simulation prior to the development of the anormal circulation feature.

Increased mesoscale variability associated with the current departure from the coast near 35 °S, is associated with an increase in the EKE signal. The model is able to reproduce the position of this coastal departure quite well, in agreement with the altimetry observations. Near the retroflection, there is a marked increase in kinetic energy. The retroflection is known to exhibit large temporal and spatial variability (Chapter 6.3). This strong mesoscale variability in the retroflection and its associated ring shedding is reflected in high EKE values in both the model and altimetry fields.

The process of eddy shedding at the retroflection and their propagation into the South Atlantic Ocean, can be seen in the form of a "fan" of EKE spreading in a general northwesterly direction from the retroflection near 18 °E into the South Atlantic Ocean. The reason for this spatial spread into the South-East Atlantic Ocean can be ascribed to variable eddy propagation directionalities, examples of which can be seen in Figure 5. HYCOM is unable to represent this spread of energy accurately, showing a tendency to favour one eddy propagation track into the South Atlantic Ocean. This seems to be a common trend among ocean general circulation models (pers. comm. Dr. Laurent Bertino, Mohn-Sverdrup Center).

Altimetry observations also show a high degree of mesoscale variability associated with the Agulhas Return Current. The topographically induced northward flow-diversion associated with the Agulhas Plateau is clearly evident in the yearly average EKE fields, and the semi-permanent downstream meanders at 29.7 °E, 35.5 °E and 42.9 °E are also represented as areas of heightened EKE, indicating the variability associated with the flow here. These areas of enhanced EKE in the Return Current are not as clearly represented in the model simulation.

Examining successive years in the HYCOM simulation, both agreements and discrepancies to the altimetry data are evident. EKE in HYCOM near the Agulhas Retroflection is comparable for years 2000, 2001 and 2002. There seems to be a focus of energy, and the spatial variability distribution is not as wide compared to observations from altimetry. In the Agulhas Current proper, with its departure from the coast, the altimetry shows a gap between the EKE associated with the south-westward flow and the north-eastward return flow around the Agulhas Plateau. This gap is not present in HYCOM. Here large features with high EKE values persist. These features extend upstream, almost to 30 °S, where EKE values from altimetry are much lower. It seems that this energy in the model arises from large anticyclonic eddies, originating in the Mozambique Channel and from the EMC, travelling downstream on the ocean side of the Agulhas Current. These eddies appear to become trapped upstream of the Agulhas Plateau. Their persistent presence in this region seems to have a significant impact on the flow regime here. The downstream circulation is adversely affected by the development of these features, the energy seems to dissipate downstream of this anormal circulation as it grows in size, eventually cutting off the downstream variability and initiating an early retroflection of the Agulhas Current (see Figure 18). This seems to be a critical issue in our and other model simulations of this region (pers. comm. Dr. Pierrick Penven, Institut de Recherche pour le Developpement; IRD).

7.2 The anormal circulation feature

Previously, we had touched on the subject of the development in the model of a large anticyclonic circulation feature, which is seemingly blocked from further downstream progression by the by the Agulhas Plateau. This anormal circulation is thought to adversely affect the throughflow between the Agulhas Plateau, causing a decrease of the Agulhas Current inflow into the Agulhas Basin, reducing the mesoscale variability usually seen here.

An analysis of the surface velocity fields from HYCOM suggests that the development and growth of this feature is associated with upstream eddies, originating in the Mozambique Channel and the EMC retroflection. The size of these eddies is extensive, up to 300 km in diameter, when these eddies connect with the current proper, they cause it to meander offshore. This meander then propagates downstream,

similarly to what is known as a Natal Pulse. Upon reaching the Agulhas Plateau, this progression is blocked and the core of the flow forced to retroflect in an anticyclonic loop. This early retroflection is aided by the anticyclonic motion of the eddy which initially induced the meander. As mentioned, it seems that the growth of this feature is attributed to upstream eddies which "pile up" in this region. The Agulhas Plateau in its northern reaches approaches depths shallower than 2500 m, and a vertical section through the anormal circulation feature (Figure 19) indicates that it reaches depths of up to 2000 m. Its progression is thus affected by its interaction with the bottom topography, which seems to prohibit its further migration downstream. It seems that the eddies generated in the Agulhas Current HYCOM are too large resulting from a lack of baroclinic gradients as discussed in Chapter 6. An additional dissipation process may to a degree reduce this feature (pers. comm. Dr. Pierrick Penven, IRD). It should be remembered that this is the first run of the model for this region, and a lot of improvements are yet to be made. The "fine-tuning" of model parameters is not within the scope of this study.

Among other possible explanations for the development of this feature is the conservation of potential vorticity, its equation given below:

$$\frac{f+\zeta}{D} = \text{const.} \tag{2}$$

where f ($= 2\Omega \sin\varphi$) is the Coriolis parameter, ζ is the relative vorticity and D, the depth. A discussion of the conservation of potential vorticity with flow over a shallow feature, follows that anticyclonic flow curvature is enhanced with the arrival of anticyclonic eddies at the Agulhas Plateau. Assuming that changes in the Coriolis parameter remain small, i.e. are negligible in zonal flow, anticyclonic eddies arriving at the Agulhas Plateau experience a vertical squeezing due to shallower bathymetry, which acts to increase the anticyclonic spin. However, the arrival of an eddy at the Agulhas Plateau should also induce a horizontal convergence, associated with the "piling up" of water behind it. This would have the opposite effect to vertical squeezing, since convergence in an eddy is associated with a depth increase, and following our previous train of thought, this would induce cyclonic flow curvature from a relative vorticity increase. It seems here, that the process of vertical squeezing is the dominant contributor to the circulation field in this region, but it does not explain the growth of this feature over time.

Boudra and Chassignet (1988) noted the development of a similar feature in their idealised, with flat bottom topography, quasi-geostrophic model experiments of the Agulhas Current and Retroflection. Their experiments show the importance of the conservation of potential vorticity and potential enstrophy in determining the retroflection strength. Winther et al. (2005) showed that the implementation of the QUICK-scheme in HYCOM improves the conservation of potential vorticity. Applying this higher order advection scheme here may have beneficial results.

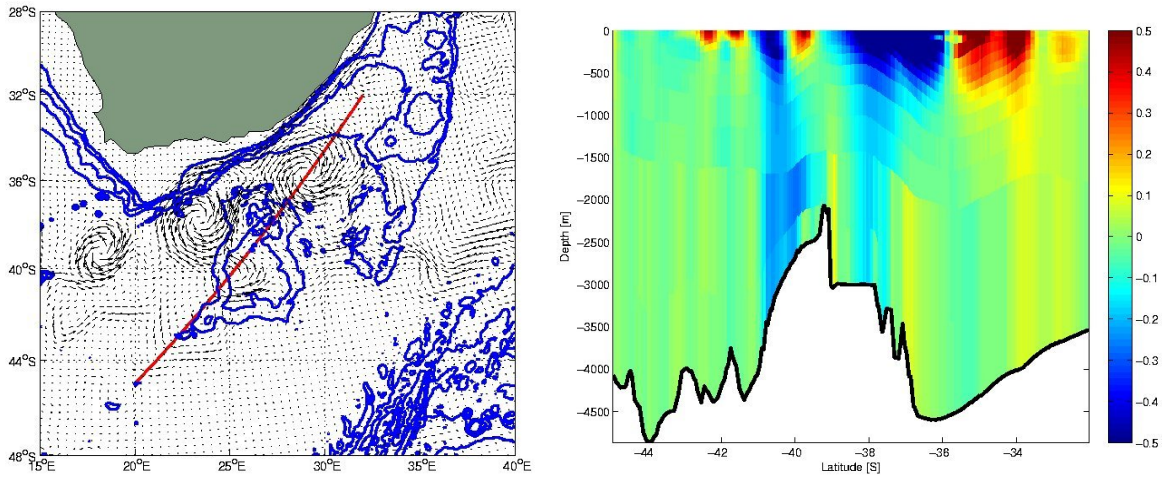

Figure 19: *HYCOM current velocities averaged for week 1 - 2002/04. Left: Surface velocity vectors from HYCOM with ocean topography (blue) and extracted section (red). Right: Vertical northward (red) and southward (blue) velocity section.*

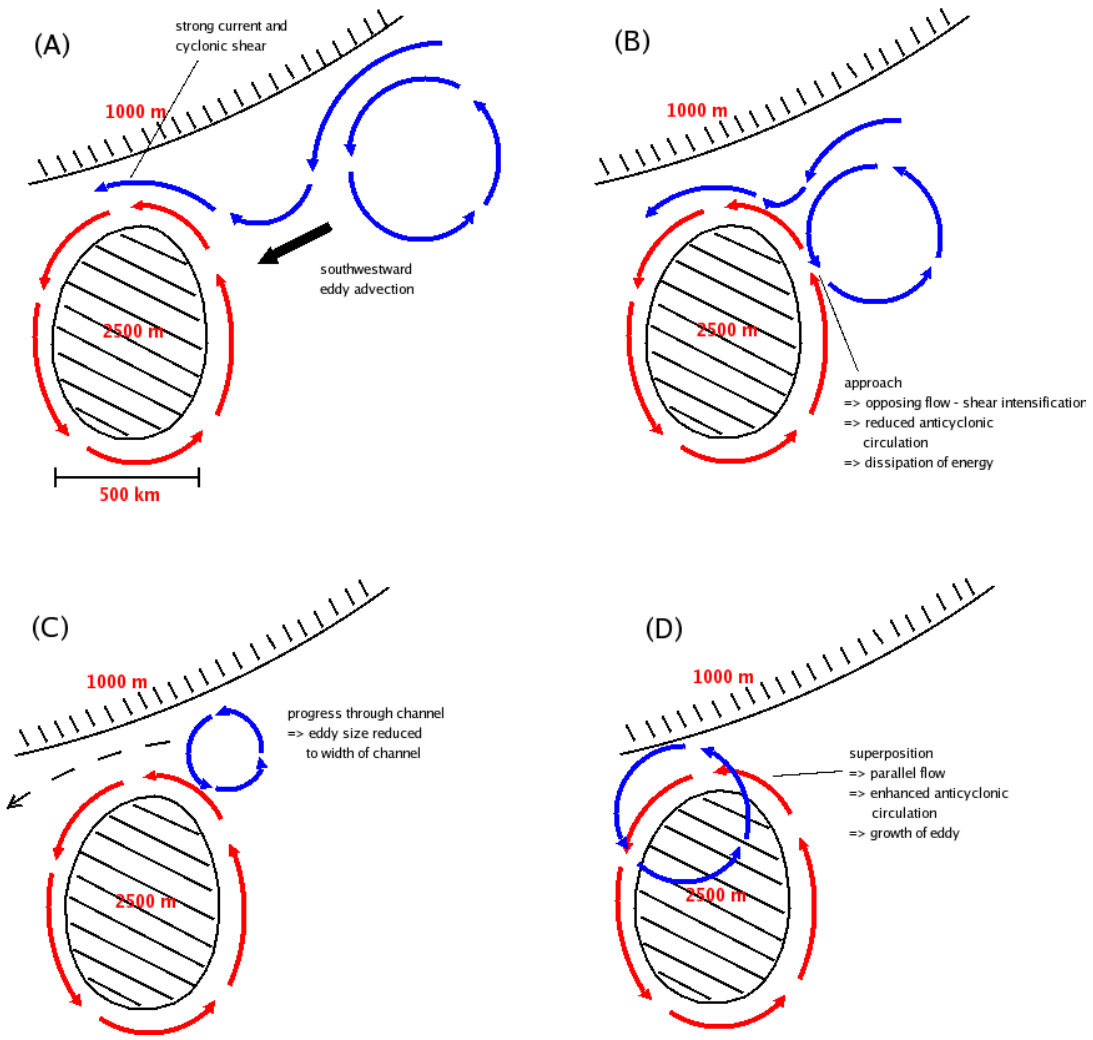

Figure 20: *Idealised representation of the flow dynamics and interaction of the background circulation at depth (red) with the upper-ocean circulation associated with approaching eddies (blue).*

A further possible explanation for the formation of this recirculation feature may be associated with the passage of eddies near the Agulhas Plateau and their interaction with the background topographically induced deep circulation around the plateau. As mentioned, the model simulation suggests that flow dynamics in the Agulhas Current are dominated by southwestward advecting eddies. In this context idealised concepts of flow dynamics at depth, derived from analyses of the model velocity fields (e.g. Figure 19) are discussed analytically (Figure 20).

The orbital flow around the Agulhas Plateau, at approximately 1500-2000 m, occurs in the model with velocities of up to 0.2 m.s^{-1}. Approaching eddies have been observed in the model to extend to depths up to 2000 m, with horizontal diameters up to 500 km (Figure 19). The velocities at depth associated with these eddies, vary between 0.1 and 0.3 m.s^{-1}, and are of similar order to the orbital flow around the Agulhas Plateau.

The following hypothesis is considered. As anticyclonic eddies arrive at the Agulhas Plateau they need to pass through a narrow channel, bordered by the Agulhas Plateau (approximately 2500 m deep) to the south and the continental shelf (1000 m deep) to the north. This channel has a width of approximately 170 km.

As the eddy approaches the Agulhas Plateau (Figure 20-A), it encounters the orbital deep circulation associated with the Agulhas Plateau, and the opposing flows result in a shear intensification (Figure 20-B). This can be seen to occur in Figure 19 (right) at approximately 2000 m depth, and 37 °S. The increased instability resulting from this shear intensification may, in turn, lead to a transfer of eddy mean energy to eddy kinetic energy at shorter scales. Hence, a gradual reduction of the eddy orbital motion and horizontal size may occur. Through such processes the eddy diameter could eventually approximate the width of

the channel and thus reach a state where its further southwestward motion through the channel is allowed (Figure 20-C).

The complex interaction between the southwestward moving eddy and the topographically steered flow around the Agulhas Plateau at around 1500 m could also influence terms in the conservation of vorticity (Equation 2), notably D and ζ. A reduction in the thickness of the eddy (D) will lead to a weakening of the vorticity (ζ) and this in turn could result in the upper part of the eddy becoming less influenced by the presence of the plateau. In such circumstances, the eddy may move over the plateau, even if its diameter is wider than the channel, allowing it to continue on its southwestward path, as shown in Figure 20-D. It is most likely that a combination of these two processes (Figure 20-C and -D) occurs in the southwestward advection of eddies.

The above described hypothesis is assumed to be repeated episodically, and can be seen to occur in the model during the first two years of the simulation. Previous estimates of anticyclonic eddy propagation velocities (Chapter 6.3; Table 2) suggest that such a propagation cycle would have a characteristic timescale of approximately 2-3 months. On the other hand, if the characteristic timescale for the blocking and interaction exceeds the period between two southwestward propagating eddies, further complication to the above picture will expectedly take place. This could involve eddy-eddy interaction as well as eddy-topographically steered flow interaction. These processes are, however, not discussed here further.

The outlined hypothesis would need more theoretical and analytical work, combined with dedicated in-situ observations, such as hydrography and more specifically, velocity measurements. Following which, one could proceed with a more reliable explanation for the complicated dynamical processes occurring in the region of the Agulhas Plateau. From this one could in turn establish improved parameterisation and constraints in numerical experiments with HYCOM.

8 Summary and conclusion

This study shows that satellite altimetry data is well suited for use in model validation and variability studies for the greater Agulhas Current system. Additionally, while altimetry provides a practical means for model validation, it is also a valuable tool in frequency, variability and propagation studies for the region. And the model simulation subsequently supported many of the findings and provided relative confidence to the assumptions made in these analyses.

Comparisons of Jason-1 along-track SLA to the gridded merged multi-mission altimeter data (Chapter 3) showed that the mesoscale variability in the Agulhas Current system is relatively slow moving in the region of the Return Current, and of the order of ∼100 km. These features should therefore be well represented in the gridded merged multi-altimeter data products. Furthermore, the comparisons of along-track data (Figures 3 and 4) to calculated *monthly mean* gridded maps (Figure 5) suggested that there was no significant loss or smoothing of information in the interpolation and production of the gridded SLA fields. Therefore, the merged maps seem to retain the temporal and spatial resolution required to resolve the mesoscale features of the greater Agulhas Current system.

The model simulation showed that these mesoscale features are also slow moving in other regions of the Agulhas Current system (Figure 8), supporting to a degree this assumption.

Following these findings, selected tracks were extracted from the gridded altimeter data and from HYCOM for the period of the model hindcast simulation, from January 2000 to December 2004 (Chapter 6.3). The Hovmoeller plots of each section (Figures 13, 14, 15 and 16) from the altimeter and model data give good qualitative comparisons, of the model simulation to the altimetry observations. A feature tracking analysis, from the Hovmoeller plots, provided initial frequency comparisons (Table 1) of each of the extracted sections. These comparisons showed that the model integration deteriorated in the last two years of the simulation experiment, and that the mesoscale variability in the Agulhas Return Current, and the eddy shedding frequency at the Agulhas Retroflection was poorly represented. The degree of discrepancy between the two data is not surprising, since this is our first attempt at simulating the region using HYCOM. Furthermore, this is a "free model run", the model parameters were not tuned, and no data assimilation was implemented in the hindcast.

Upstream in the northern Agulhas Current, the model simulation is much better. The model fields strongly suggest a connection of the anticyclonic eddies observed in the ocean side of the Agulhas Current proper to the Mozambique Channel eddies. These findings are further confirmed in our analysis of the altimetry data for this region. It was shown in both the model simulation and altimetry observations, that mesoscale features originating in the Mozambique Channel appear to interact with the northern Agulhas Current up to 90% of the time, and of these almost 80% seemingly further interact at the Agulhas Retroflection. The percentage calculated from the model simulation for the case of Mozambique Channel eddies interacting at the Retroflection is lower, but a connection is clearly evident in the simulation. This frequency underestimate evident in HYCOM can be explained by the appearance of a recirculation feature in the model, as was discussed in Chapter 7.2.

Following the frequency analysis from the Hovmoeller plots, feature propagation velocities were determined (Table 2), for various sub-regions of the extracted sections. The propagation estimates agree well with available literature to date, providing confidence in the validity of the approach used in this analysis. Furthermore for the Agulhas Current system, this indicates that the SLA data products as provided by CLS are usable in such analysis, without the need for additional conditioning of the data such as applying advanced filtering functions.

To quantify the frequency estimates given in Table 1 a Fourier analysis was applied at each geographical point along the extracted sections. Their interpretation is complicated, showing a range of various frequencies in the different sections. Nevertheless, they strongly support the initial frequency estimates from the feature tracking analysis.

In the section extracted for the Agulhas Current (Figure 13), the power spectrum in the model simulation clearly suggests a connection of the Mozambique Channel eddies to the northern Agulhas Current, evident in the 5 yr^{-1} peak. The connection is less evident in the altimetry power spectrum, but a degree of upstream correlation seems evident.

Regarding the eddy shedding frequency at the Agulhas Retroflection, and their propagation into the South Atlantic Ocean along various paths, combining the feature tracking analysis and supporting it with

Fourier analysis, provides realistic estimates. From these, Agulhas Rings were estimated to be shed 5-6 times per year during our analysis period, with a preference to drift along the west-northwest section (Figure 15). The preference for this section is also evident in the model simulation, however HYCOM was unable to simulate a more variable eddy corridor, and the ring shedding frequency was lower, especially in the last two years of the simulation associated with the development of the afore mentioned model artifact.

To obtain a broader spatial comparison of the altimetry and model data, eddy kinetic energy (EKE) was calculated from altimetry and HYCOM SLA data for successive years (Figures 17 and 18). Regions of enhanced EKE can clearly be seen associated with the strong mesoscale variability of the Mozambique Channel, the East Madagascar Current retroflection, the Agulhas Current, the Agulhas Return Current and especially in the Agulhas Retroflection region.

The general distribution of the EKE for the greater Agulhas system is relatively well represented in the model simulation. Both the altimetry and model EKE suggest a connection with the mesoscale variability of the Mozambique Channel, the East Madagascar Current Retroflection and the Agulhas Current, further supporting our previous findings. However, the model clearly over-estimates the EKE in the region between 30 °S and 40 °S and 15 °E and 30 °E, and a clear preference for the west-northwest eddy track is evident. The development of the model artifact can already be seen in the years leading up to its "full" development and subsequent downstream variability decrease, toward the end of year 2002. The last two simulation years, 2003 and 2004 (Figure 18), show that the model artifact has grown to such an extent that the downstream variability has essentially shut down.

As mentioned this model artifact is held responsible for the poor representation of mesoscale variability in the Agulhas Retroflection, the Agulhas Return Current, and that HYCOM ring shedding frequency is too low. Additional adverse implications of this feature can be seen in the general circulation features of our model simulation (Chapter 6). Where the Agulhas Retroflection can be seen to have retreated to almost 30 °E (Figure 7, right) in strong disagreement to previous literature and present observations. Furthermore, its affect on the salinity field from GoodHope II (Figure 10) is clearly evident, with the absence of the saline water advection from the Agulhas Current into the South Atlantic Ocean. The SST fields also show this discrepancy (Chapter 6.2).

An analysis of model velocity fields (Chapter 7.2) suggests that this feature develops as a result of a blocking of the eddy passage through the channel between the Agulhas Plateau and the continental shelf. However, its appearance is yet to be more clearly determined, and is of importance in numerical modelling of this region since its development has been noted in various other Ocean General Circulation Models (pers. comm. Dr. Pierrick Penven, IRD). Further simulation experiments and collaborative studies with other ocean modelling groups are required to adequately resolve this issue.

It remains, that much of the discrepancies evident in our model simulation cannot fully be explained by altimetry observations alone, and a more in depth assessment of the vertical structure is required to achieve this. In a region where only sparse hydrographic data is available, and almost none during the period from January 2000 to December 2004, this is a very challenging task.

To summarise and conclude, the main findings of this study are highlighted again below:

- The gridded merged SLA data is well suited for describing the mesoscale variability in the Agulhas Current system, and thus in model validation and variability studies.
- The validation approach, using Fourier analysis, gives a statistical comparison of the model and altimetry fields.
- The model simulates the mesoscale variability in the Northern Agulhas Current well.
- Simulation of the more variable regions, namely the Agulhas Retroflection and associated ring shedding, is problematic.
- The power spectra from the Fourier analysis describe a range of frequencies in the Agulhas Current system, supporting the initial feature tracking analysis. The following conclusions were drawn from these:
  - Strong indication of seasonal signals in the Agulhas Current.

  - Intra-seasonal signal of the Agulhas Current evident in altimetry but not in the model fields, the source remains unexplained.
  - Enhanced seasonal signals associated with the semi-permanent meanders of the Agulhas Return Current is evident in the altimetry.
  - Range of eddy frequencies evident.
  - Strong suggestion that mesoscale eddies from the Mozambique Channel interact frequently at the Retroflection, approximately 70% of the time.
  - These Mozambique Channel eddies occur at a frequency of 5 yr^{-1}.
  - Surprisingly regular east-west oscillating Retroflection, 6 yr^{-1}.
  - Estimate of Agulhas Ring shedding events occurring 5-6 yr^{-1}, in good agreement with previous literature.

- Many of the findings are supported by the model simulation.
- Outstanding: adequate explanation for the appearance and development of the model artifact.

The first attempt at modelling the Agulhas Current system using a regional model of HYCOM, yields promising results. There are still improvements to be made and this is seemingly a very difficult region to model, since various other Ocean General Circulation Models develop some form of this anticyclonic recirculation feature.

To conclude, the main focus of this study has been to validate the model simulation in HYCOM from satellite altimetry, and it was shown that this was achieved in a qualitative as well as quantitative way.

References

Ansorge, I. J., Speich, S., Lutjeharms, J. R. E., Rautenbach, C. J. W., Froneman, P., Rouault, M., and Garzoli, S. (2005). Monitoring the oceanic flow between Africa and Antarctica: Report of the first GoodHope cruise. *S. Afr. J. Sci.*, 101(1-2):29–35.

Batlak, B. B. (2005). Indian Ocean: Validation of the Hybrid Coordinate Ocean Model. Mohn-Sverdrup Center; Technical Report No. 262.

Belkin, I. M. and Gordon, A. L. (1996). Southern Ocean fronts from Greenwich meridian to Tasmania. *J. Geophys. Res.*, 101(C2):3675–3696.

Bentsen, M., Evensen, G., Drange, H., and Jenkins, A. D. (1999). Coordinate transformation on a sphere using conformal mapping. *Mon. Weather Rev.*, 127:2733–2740.

Biastoch, A. and Krauss, W. (1999). The role of mesoscale eddies in the source regions of the Agulhas Current. *J. Phys. Oceanogr.*, 29:2303–2317.

Bleck, R. (2002). An oceanic general circulation model framed in hybrid isopycnic-Cartesian coordinates. *Ocean Modelling*, 37:55–88.

Bleck, R. and Smith, L. (1990). A wind-driven isopycnic coordinate model of the North Atlantic and Equatorial Atlantic Ocean. 1: Model development and supporting experiments. *J. Geophys. Res.*, 95:3273–3285.

Boebel, O., Lutjeharms, J. R. E., Schmid, C., Zenk, W., Rossby, T., and Barron, C. (2003a). The Cape Couldron: a regime of turbulent inter-ocean exchange. *Deep-Sea Res. (II Top. Stud. Oceanogr.)*, 50:57–86.

Boebel, O., Rossby, T., Lutjeharms, J. R. E., Zenk, W., and Barron, C. (2003b). Path and variability of the Agulhas Return Current. *Deep-Sea Res. (II Top. Stud. Oceanogr.)*, 50:35–56.

Boudra, D. B. and Chassignet, E. P. (1988). Dynamics of Agulhas Retroflection and Ring Formation in a Numerical Model. Part I: The Vorticity Balance. *J. Phys. Oceanogr.*, 18:280–303.

B.P.Leonard (1979). A stable and accurate convective modelling procedure based on quadratic upstream interpolation. *Comp. Methods Appl. Mech. Eng.*., 19:59–98.

Bracewell, R. (1999). *The Fourier Transform and Its Application.* New York: McGraw-Hill.

Browning, G. L. and Kreiss, H. O. (1982). Initialization of the shallow water equations with open boundaries by the bounded derivative method. *Tellus*, 34:334–351.

Browning, G. L. and Kreiss, H. O. (1986). Scaling and computation of smooth atmospheric motions. *Tellus*, Ser. A 38:295–313.

Bryden, H. L., Beal, L. M., and Duncan, L. M. (2005). Structure and Transport of the Agulhas Current and Its Temporal Variability. *J. Oceanogr.*, 61:479–492.

Davies, H. C. (1983). Limitations of some common lateral boundary schemes used in NWP models. *Mon. Weather Rev.*, 111:1002–1012.

de Ruijter, W. P. M., Ridderinkhof, H., Lutjeharms, J. R. E., Schouten, M. W., and Veth, C. (2002). Observations of the flow in the Mozambique Channel. *Geophys. Res. Lett.*, 29(10):1502–1504.

de Ruijter, W. P. M., van Aken, H. M., Beier, E., Lutjeharms, J. R. E., Matano, R. P., and Schouten, M. W. (2004). Eddies and dipoles around South Madagascar: formation, pathways and large-scale impact. *Deep-Sea Res.*, 51:383–400.

Ducet, N., Traon, P. Y. L., and Reverdin, G. (2000). Global high-resolution mapping of ocean circulation from TOPEX/Poseidon and ERS-1 and -2. *J. Geophys. Res.*, 105:19477–19498.

Feron, R. C. V., de Ruijter, W. P. M., and Oskam, D. (1992). Ring shedding in the Agulhas Current System. *J. Geophys. Res.*, 97:9467–9477.

Garzoli, S. L., Gordon, A. L., Kamenkovich, V., Pillsbury, D., and Duncombe-Rae, C. (1996). Variability and sources of the southeastern Atlantic circulation. *J. Mar. Res.*, 54:1039–1071.

Gordon, A. L. (1985). Indian-Atlantic transfer of thermocline water at the Agulhas Retroflection. *Science*, 227:1030–1033.

Gründlingh, M. L. (1983). On the course of the Agulhas Current. *S. Afr. Geograph. J.*, 65:49–57.

Holland, W. R., Chow, J., and Bryan, F. (1998). Application of a third-order upwind scheme in the NCAR ocean model. *J. Clim.*, 11:1487–1493.

Large, W. G., McWilliams, J. C., and Doney, S. C. (1994). Oceanic vertical mixing: A review and a model with a nonlocal boundary layer parameterization. *Rev. of Geophys.*, 32:363–403.

Legates, D. and Willmott, C. (1990). Mean seasonal and spatial variability in gauge-corrected, global precipitation. *J. Clim.*, 10:111–127.

Lutjeharms, J. R. E. (1985). Location of frontal systems between Africa and Antarctica: some preliminary results. *Deep-Sea Res.*, 32(12):1499–1509.

Lutjeharms, J. R. E. (2006). *The Agulhas Current.* Springer-Praxis Books, to be published in August.

Lutjeharms, J. R. E. and Ansorge, I. (2001). The Agulhas Return Current. *J. Mar. Sys.*, 30:115–138.

Lutjeharms, J. R. E., Bang, N. D., and Duncan, C. P. (1981). Characteristics of the currents east and south of Madagascar. *Deep-Sea Res.*, 28:879–899.

Lutjeharms, J. R. E., Catzel, R., and Valentine, H. R. (1989). Eddies and other border phenomenon of the Agulhas Current. *Cont. Shelf Res.*, 9:597–616.

Lutjeharms, J. R. E., Mey, R. D., and Hunter, I. T. (1986). Cloud lines over the Agulhas Current. *S. Afr. J. Sci.*, 82:635–640.

Lutjeharms, J. R. E. and Roberts, H. R. (1988). The Natal Pulse: An extreme transient on the Agulhas Current. *J. Geophys. Res.*, 93:631–645.

Lutjeharms, J. R. E. and Valentine, H. R. (1984). Southern Ocean thermal fronts south of Africa. *Deep-Sea Res.*, 31(12):1461–1475.

Lutjeharms, J. R. E. and van Ballegooyen, R. C. (1988). The retroflection of the Agulhas Current. *J. Phys. Oceanogr.*, 18:1570–1583.

Lutjeharms, J. R. E., Wedepohl, P. M., and Meeuwis, J. M. (2000). On the surface drift of the East Madagascar and the Mozambique Currents. *S. Afr. J. Sci.*, 96:141–147.

Maltrud, M. E., Smith, R. D., Semtner, A. J., and Malone, R. C. (1998). Global eddy-resolving ocean simulations driven by 1985-1995 atmospheric winds. *J. Geophys. Res.*, 103(30):825–830,853.

Matano, R. P., Beier, E. J., and Strub, P. T. (2001). Large-Scale Forcing of the Agulhas Variability: The Seasonal Cycle. *J. Phys. Oceanogr.*, 32:1228–1241.

Matano, R. P., Simionato, C. G., de Ruijter, W. P. M., van Leeuween, P. J., Strub, P. T., Chelton, D. B., and Schlax, M. G. (1998). Seasonal variability in the Agulhas Retroflection region. *Geophys. Res. Lett.*, 25(23):4361–4364.

Minster, J. F. and Gennero, M. C. (1995). High-frequency variability of western boundary currents using ERS-1 three-day repeat altimeter data. *J. Geophys. Res.*, 100:22603–22612.

Olson, D. B. and Evans, R. H. (1986). Rings of the Agulhas Current. *Deep-Sea Res.*, 33:27–42.

Pichevin, T., Nof, D., and Lutjeharms, J. R. E. (1999). Why are there Agulhas Rings. *J. Phys. Oceanogr.*, 29(4):693–707.

Pond, S. and Pickard, G. L. (1983). *Introductory Dynamical Oceanography.* Elsevier Butterworth-Heinemann.

Quartly, G. D. and Srokosz, M. A. (2002). SST observations of the Agulhas and East Madagascar Retroflections by the TRMM Microwave Imager. *J. Phys. Oceanogr.*, 32(5):1585–1592.

Ridderinkhof, H. and de Ruijter, W. P. M. (2003). Moored current observations in the Mozambique Channel. *Deep-Sea Res. (II Top. Stud. Oceanogr.)*, 50:1933–1955.

Robinson, I. S. (2004). *Measuring the Oceans from Space; The principles and methods of satellite oceanography.* Springer-Praxis Books in Geophysical Sciences.

Rouault, M. and Lutjeharms, J. R. E. (2003). Estimation of Sea Surface Temperature around southern Africa from satellite derived microwave observations. *S. Afr. J. Sci.*, 99:489–493.

Rouault, M., Verley, P., and Backeberg, B. (2006). Ocean-atmosphere interaction above Agulhas Current eddies. Submitted to Deep-Sea Res. (II Top. Stud. Oceanogr.).

Sætre, R. (1985). Surface currents in the Mozambique Channel. *Deep-Sea Res.*, 32:1457–1467.

Sætre, R. and da Silva, A. J. (1984). The circulation of the Mozambique Channel. *Deep-Sea Res.*, 31:485–508.

Schouten, M. W., de Ruijter, W. P. M., and van Leeuwen, P. J. (2002). Upstream control of Agulhas Ring shedding. *J. Geophys. Res.*, 107(C8):3109–3120.

Slutz, R., Hiscox, S. L. J., Woodruff, S., Jenne, R., Joseph, D., Steurer, P., and Elms, J. (1985). Comprehensive ocean-atmosphere dataset; Release 1. Tech. Rep. NTIS PB86-105723, NOAA Environmental Research Laboratories, Climate Research Program, Boulder, CO.

SSALTO/DUACS User Handbook (2004). *(M)SLA and (M)ADT Near-Real Time and Delayed Time Products.* Version 1rev3.

Stramma, L. and Lutjeharms, J. R. E. (1997). The flow field of the subtropical gyre in the South Indian Ocean. *J. Geophys. Res.*, 99:14053–14070.

Teague, W. J., Carron, M., and Hogan, P. J. (1990). A comparison between the Generalized Digital Environmental Model and Levitus climatologies. *J. Geophys. Res.*, 95(C5):7167–7183.

Traon, P. Y. L. and Dibarboure, G. (1999). Mesoscale mapping capabilities of multiple-satellite altimeter missions. *J. Atmos. Ocean. Technol.*, 16:1208–1223.

van Leeuwen, P. J., de Ruijter, W. P. M., and Lutjeharms., J. R. E. (2000). Natal Pulses and the formation of Agulhas Rings. *J. Geophys. Res.*, 105:6425–6436.

Wang, L. and Koblinsky, C. J. (1996). Low-frequency variability in the region of the Agulhas Retroflection. *J. Geophys. Res.*, 101:3597–3614.

Webb, D. J., Cuevas, B. D., and Richmond, C. (1998). Improved advection schemes for ocean models. *J. Atmos. Ocean Tech.*, 15:1171–1187.

Weeks, S. J., Shillington, F. A., and Brundrit, G. B. (1998). Seasonal and spatial SST variability in the Agulhas retroflection and Agulhas return current. *Deep-Sea Res.*, 45:1611–1625.

Winther, N. and Evensen, G. (2006). A hybrid coordinate ocean model for shelf sea simulation. *Ocean Modelling*, 13:221–237.

Winther, N. G., Morel, Y., and Evensen, G. (2005). Efficiency of high order numerical schemes for momentum advection. Submitted to J. Mar. Sys.